Supplementary Materials for

Selective and cross-reactive SARS-CoV-2 T cell epitopes in unexposed humans

Jose Mateus, Alba Grifoni, Alison Tarke, John Sidney, Sydney I. Ramirez, Jennifer M. Dan, Zoe C. Burger, Stephen A. Rawlings, Davey M. Smith, Elizabeth Phillips, Simon Mallal, Marshall Lammers, Paul Rubiro, Lorenzo Quiambao, Aaron Sutherland, Esther Dawen Yu, Ricardo da Silva Antunes, Jason Greenbaum, April Frazier, Alena J. Markmann, Lakshmanane Premkumar, Aravinda de Silva, Bjoern Peters, Shane Crotty, Alessandro Sette*†, Daniela Weiskopf*†

*Corresponding author. Email: alex@lji.org (A.S.); daniela@lji.org (D.W.)
†These authors contributed equally to this work.

Published 4 August 2020 on *Science* First Release
DOI: 10.1126/science.abd3871

This PDF file includes:

Other Supplementary Material for this manuscript includes the following:
(available at science.sciencemag.org/cgi/content/full/science.abd3871/DC1)

MDAR Reproducibility Checklist

Materials and Methods

Human blood samples

Healthy unexposed donors

For the epitope identification studies, a total of 18 peripheral blood samples were obtained from local healthy adult blood donors in an anonymous fashion. Both sexes were represented (5:12, M:F, 1 unknown) and donors ranged from 21 to 66 years of age (average 36 years). All protocols described herein were approved by the institutional review boards (IRB) of the La Jolla Institute (IRB#:VD-112). Blood samples were obtained between 2015 and 2018, thereby excluding the possibility that the donors were exposed to SARS-CoV-2, since the virus was not yet circulating in the United States. Collection and processing of blood samples was performed as previously described (*37*). Seronegativity against SARS-CoV-2 was confirmed by ELISA as described below and shown in **Fig. S1A**. At the time of enrollment in the initial studies, all individual donors provided informed consent that their samples could be used for future studies, including this study. Donor characteristics and HLA phenotype of donors utilized for epitope identification are listed in **Table S6.**

To confirm the identified epitopes in an independent cohort, we utilized 25 peripheral blood samples that had been collected from local healthy donors before 2015, excluding previous exposure to SARS-CoV-2. For samples collected in 2020, seronegativity was confirmed by SARS-CoV-2 ELISA **(Fig. S1A).** Also, in this cohort, both sexes were represented (9:14, M:F, 2 unknown) and donors ranged from 25 to 67 years of age (average 40 years). Details of this unexposed donor cohort utilized to verify cross-reactivity are shown in **Table S4.**

Convalescent COVID-19 donors

Blood from convalescent donors was either obtained at a UC San Diego Health clinic under the approved IRB protocols of the University of California, San Diego (UCSD; 200236X) or recruited at the La Jolla Institute under IRB approved (LJI; VD-214). Convalescent donors were California residents, who were either referred to the study by a health care provider or self-referred. A third cohort of COVID convalescent donors was provided by the CRO Sanguine that collected blood from previously PCR+ confirmed donors after resolution of symptoms. In the overall cohort, both sexes were represented (11:9, M:F) and donors ranged from 32 to 63 years of age (average 48 years). Blood was collected in acid citrate dextrose (ACD) tubes (UCSD) or in EDTA tubes (LJI and Sanguine) and stored at room temperature prior to processing for PBMC isolation and plasma collection. Seropositivity against SARS-CoV-2 was confirmed by ELISA, as describe below and shown in **Fig. S1A**. Details of this convalescent COVID cohort utilized to verify cross-reactivity are listed in **Table S5.** At the time of enrollment, all convalescent COVID-19 donors provided informed consent to participate in the present and future studies.

Peripheral blood mononuclear cells (PBMCs) and plasma isolation

Whole blood was collected in heparin coated blood bags (healthy unexposed donors) or in ACD tubes (COVID-19 donors) and centrifuged for 15 min at 1850 rpm to separate the cellular fraction and plasma. The plasma was then carefully removed from the cell pellet and stored at -20C. PBMCs were isolated by density-gradient sedimentation using Ficoll-Paque (Lymphoprep, Nycomed Pharma, Oslo, Norway) as previously described (*21*). Isolated PBMC were cryopreserved in cell recovery media containing 10% DMSO (Gibco), supplemented with 10%

heat inactivated fetal bovine serum (FBS; Hyclone Laboratories, Logan UT) and stored in liquid nitrogen until used in the assays.

Serology

SARS-CoV-2 ELISA

SARS-CoV-2 seropositivity in convalescent COVID-19 donors was determined as previously described (*4, 38*). Briefly, Corning 96-well half-area plates (ThermoFisher 3690) were coated with 1 µg/mL SARS-CoV-2 RBD overnight at 4°C. The next day plates were blocked day with 3% milk (Skim Milk Powder ThermoFisher LP0031 by weight/volume) in Phosphate Buffered Saline (PBS) containing 0.05% Tween-20 (ThermoScientific J260605-AP) for 2 hours at room temperature. Heat-inactivated plasma was then added to the plates and incubated for 1.5 hours at room temperature **(Fig. S1A)**.

OC43, NL63 HKU1 and SARS-CoV2 ELISA

An in-house ELISA at UNC was performed by coating with recombinant S RBD antigens (HCoV OC43, HCoV NL63 and HCoV HKU1) in TBS for 1 h at 37 C as previously described (*33*). After blocking, we added 1:20 diluted serum and incubated at 37°C for 1 h. Antigen-specific antibodies (Ig) were measured at 405 nm by using alkaline phosphatase conjugated goat anti-human IgG and 4-Nitrophenyl phosphate **(Fig. S1B)**.

HLA typing and phenotype frequency calculations

HLA typing was performed by an ASHI-accredited laboratory at Murdoch University (Western Australia) for Class I (HLA A; B; C) and Class II (DRB1, DRB3/4/5, DQA1/DQB1, DPB1), as previously described (15, 22, 23) (**Table S6**). To ensure that our cohort was representative of the general population, we compared frequencies of the main HLA class II alleles observed in our donor cohort with the those observed in our repository of over 3,500 donors, reflecting a variety of clinical studies and a diverse set of ethnicities, ranging from the USA, South and Central America, Asia, South Africa and Europe (**Fig. S3**).

In general, the HLA representation was similar in the two populations. Of the 21 different HLA class II alleles identified in our cohort with phenotypic frequencies >10%, 15 (71%) are also present in the general population with frequencies >10%. At the same time, 22 (81%) of the 27 alleles included in a reference panel of the most common and representative class II alleles in the general population (*39*) are also present in the cohort studied here. The four most common DRB1 alleles in the cohort (DRB1*07:01, DRB1*01:01, DRB1*11:01 and DRB1*15:01), present with frequencies of 15% or greater, are also found in the worldwide population with frequencies >8%. Similar correspondence was also noted at the DRB3/4/5 and DQB1 and DPB1 loci. These results indicate that the majority of the HLA class II alleles most frequent worldwide are also well represented in our donor cohort, and vice versa.

Epitope predictions and peptide selection

We previously predicted SARS-CoV-2 CD4 T cell epitopes utilizing the Immune Epitope Database and Analysis Resource (IEDB)(*4*). We have also previously developed the Megapool (MP) approach to allow simultaneous testing of large number of epitopes. According to this

approach large numbers of different epitopes are solubilized, pooled and re-lyophilized to avoid cell toxicity problems associated with high concentrations of DMSO typically encountered when single pre-solubilized epitopes are pooled (*40*). These MPs have been used in a number of indications, including allergies (*41*), tuberculosis (*42*), tetanus, pertussis (*43, 44*) and DENV for both $CD4^+$ and $CD8^+$ T cell epitopes (*21, 45, 46*).

Here we utilized a MP of 253 overlapping peptides spanning the entire sequence of the spike protein. Of note, the receptor binding domain (RBD) only accounts for a small portion of the S protein (defined as residues 319-541 (*38*)). In parallel we predicted dominant CD4 from the remainder of the SARS-CoV-2 genome and accordingly produced a second MP, corresponding to 246 HLA class II CD4 epitopes as previously described (*4*). We have previously shown that these megapools are suitable to stimulate T cell responses from either exposed or unexposed individuals, and expanding the existing repertoire of T cell specificities (*19, 46, 47*). For screening purposes and intermediate deconvolution, each of the two MP used for stimulation was further subdivided in 25 (S) and 22 (R) mesopools of 10 to 11 peptides each.

FluoroSPOT assays on short term TCLs

In vitro expansion of SARS-COV-2 specific T cells for mesopools evaluation

$12x10^6$ PBMC s were stimulated with SARS-CoV-2-specific megapools kept at 37◦C in 5% CO_2, IL-2 (10 U/mL; eBioscience) was added at 4, 7, 11 and 14 days after initial antigenic stimulation and harvested on day 14 or 17. Harvested cells were counted and triplicates of 5×10^4 PBMCs were incubated in the presence of the SARS-CoV-2 mesopools used for stimulation [1 µg/mL of each peptide] (on day 14) or with the individual peptide contained in the positive pools assayed at day 14 were used for stimulation [1 µg/mL] (on day 17). In both cases, no additional APC were added to the culture and after 20 hours of incubation at 37◦C, cells were incubated with IFNγ mAb (7-B6-1-BAM Mabtech, Stockholm, Sweden) and IL-5 mAb (5A10-WASP Mabtech, Stockholm, Sweden) for 2 hours and developed as previously described (7, 14).

In vitro expansion of SARS-COV-2 specific T cells for peptide evaluation

Short-term cell lines for 14 days were set up using donors that were utilized in the epitope identification screen. $12x10^6$ PBMC were expanded using the specific SARS-CoV-2 epitope/donor [1 µg/mL] combinations selected on the basis of the primary screen. IL-2 was added day on day 3, 7, and 11. After 14 days, IFNγ/ Il-5 FluoroSpot assays were performed as described above. Briefly, each TCL was tested with the SARS-CoV-2 epitope used for stimulation and peptides corresponding to analogous sequences from other HCoV. Each peptide was tested at six different concentrations (1 µg/mL, 0.1 µg/mL, 0.01 µg/mL, 0.001 µg/mL, 0.0001 µg/mL, 0.00001 µg/mL) by incubating it for 20 hours at 37 C, 5% CO_2 at a concentration of $1x10^5$ cells/mL.

For the experiments in **Fig. S8**, we pre-sorted naïve ($CD45RA^+$ $CCR7^+$) and memory $CD4^+$ T cells ($CD45RA^-$ $CCR7^{+/-}$) utilizing a FACS Aria III sorter. Sorted $CD3^-$ cells were added to the cultures at a 1:2 ratio as antigen presenting cells [$2x10^6$:$4x10^6$ cells]. Whole PBMC cultures were also set up as a positive control. All cultures were stimulated CD4-[S31] epitope pool at 1 µg/mL. After 14 days, responses to the CD4-[S31] epitope pool were assessed as described above.

Flow cytometry assays

Intracellular cytokine staining (ICS) assay for positive mesopools

Intracellular staining was performed as previously described (*4*). Based on FluoroSPOT results on day 14, expanded cells at day 17 were cultured for 6 hours in the presence of the specific positive mesopools [1 μg/mL] in 96-wells U bottom plates at 0.5-1x10^6 PBMCs per well. An equimolar volume of DMSO was used as negative control. Golgi-Plug containing brefeldin A (BD Biosciences, San Diego, CA) was added 1 hour into the culture. At the end of the 6 hours of stimulation, cells were stained with surface markers for 30 min at 4°C followed by fixation with 4% paraformaldehyde (Sigma-Aldrich, St. Louis, MO) at 4°C for 10 min. Intracellular staining was incubated at room temperature for 30 min after cells permeabilization with saponin. The gates applied for the identification of IFNγ production on the total population of $CD4^+$ or $CD8^+$ T cells were defined according to the cells cultured with DMSO for each individual. Intracellular staining was incubated at RT for 30 min after cells permeabilization with saponin. The antibody panel utilized in the ICS staining is shown in **Table S7.**

Activation induced markers (AIM) assay for pool responses and memory phenotype

Cells were cultured for 24 hours in the presence of HCoV or SARS-CoV-2 specific MPs [1 μg/mL] or phytohemagglutinin [5 μg/mL] (PHA, Roche) in 96-wells U bottom plates at 1x10^6 PBMCs per well, as previously described (*4*). A stimulation with an equimolar amount of DMSO was performed as negative control, PHA, and stimulation with a combined CD4 and CD8 cytomegalovirus MP (CMV, 1 μg/mL) were included as positive controls. The antibody panel utilized in the AIM staining is shown in **Table S8.**

Sequence analysis for commonly circulating coronaviruses.

For the 229E, NL63, HKU1 and OC43 common coronaviruses, we obtained protein sequences from GenBank records for complete genome sequences annotated as being the RefSeq for the corresponding virus; 229E: https://www.ncbi.nlm.nih.gov/nuccore/12175745; NL63: https://www.ncbi.nlm.nih.gov/nuccore/49169782; HKU1: https://www.ncbi.nlm.nih.gov/nuccore/85667876; OC43: no RefSeq record was available, so we used the complete genome record https://www.ncbi.nlm.nih.gov/nuccore/AY391777.1, as it contained annotation indicating it was the 'prototype strain'. 229E has entries for both the orf1ab and orf1a proteins, where the latter is shorter and largely nested sequence, differing only in the last 9 residues, and was removed to avoid duplicate hit counts. All of the 15-mer peptides from SARS-CoV-2 that were tested for immunogenicity in SARS-CoV-2 unexposed donors were compared against every position in the protein sequences from these commonly circulating coronaviruses described above to find the best matching sequence regions. For each peptide, we then calculated the average percent sequence identify across the four viruses and the maximum percent sequence identify for a given peptide in any of the four viruses.

In an alternative and broader approach, we gathered protein sequences from Alphacoronaviruses (a genus which includes 229E and NL63) and from Embecoviruses, (a sub-genus of Betacoronaviruses that includes the commonly circulating OC43 and HKU1 viruses, but excludes SARS-CoV-1, SARS-CoV-2 and MERS viruses). All of the 15-mer peptides from SARS-CoV-2 that were tested for immunogenicity in SARS-CoV-2 unexposed donors were compared against the protein sequences from these coronaviruses to find matching sequence

regions, allowing up to 3 mismatches. All selected epitopes and the respective HCoV variants are listed in **Table S2 and S3**.

Putative HLA restriction determination

Putative HLA class II restrictions of the identified epitopes were inferred based on NetMHCIIpan binding predictions, as previously validated on the basis of an analysis of HLA restrictions for TB and Shingrix epitopes (*22, 42*). More specifically, for each epitope-donor combination, DRB1 and DQ putative restrictions were assigned by examining the alleles expressed in each particular donor and the predicted binding capacity of the corresponding responding epitope, and then calling a potential restriction if one or more of the expressed alleles is predicted to bind at 25^{th} percentile rank level, or better. This procedure has been shown to efficiently capture about 60% of the experimentally determined DRB1 and DQ restrictions, while having marginal predictive power to assign DP or DRB3/4/5 restrictions (*22, 42*).

Statistical analysis

Data and statistical analyses were done in FlowJo 10 and GraphPad Prism 8.4, unless otherwise stated. The statistical details of the experiments are provided in the respective figure legends. Data plotted in linear scale were expressed as Mean ± Standard Deviation (SD). Data plotted in logarithmic scales were expressed as Geometric Mean ± Geometric Standard Deviation (SD). Mann-Whitney or Wilcoxon tests were applied for unpaired or paired comparisons, respectively. Details pertaining to significance are also noted in the respective legends.

Supplementary figures

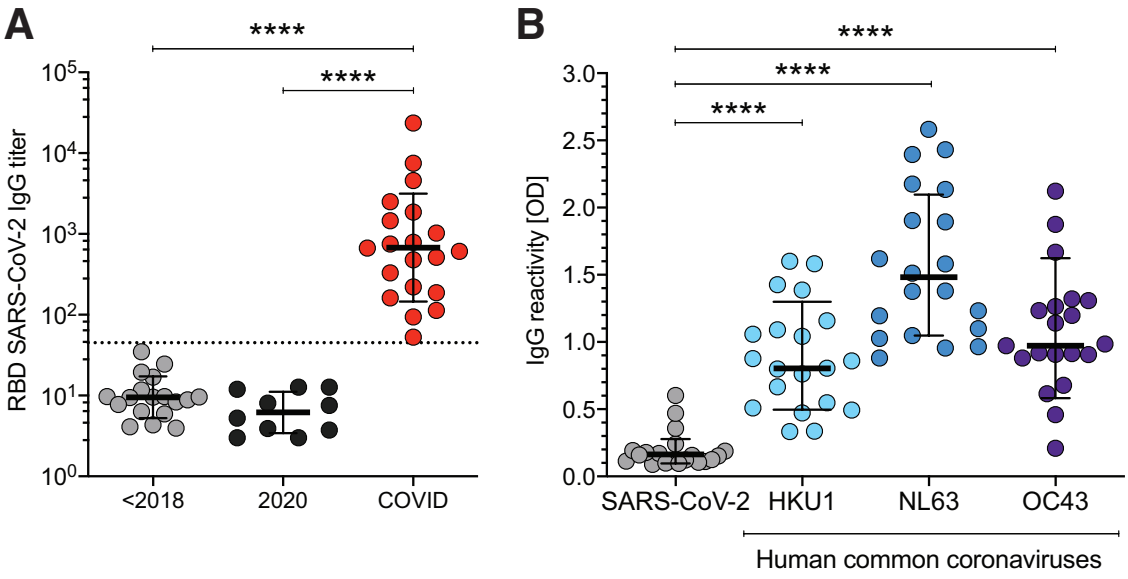

Figure S1. IgG titers against SARS-CoV-2 and HCoVs.

(A) Plasma ELISA titers for IgG are shown for unexposed donors collected before 2018 n=18 (grey balls, see also Table S4), unexposed donors collected in 2020 (n=18, black balls, see also Table S4) and donors exposed to SARS-CoV-2 (n=20, red balls, see also Table S5) are shown. Dotted line indicated limit of positivity. (B) Spike RBD antigen binding (expressed as OD) from SARS-CoV-2 (gray balls), HKU1 (light blue balls), NL63 (blue balls), and OC43 (dark blue balls) were assessed by in-house ELISA assay in SARS-CoV-2-unexposed samples collected before 2018 (see also Table S4). Black bars indicate the geometric mean and geometric SD. Statistical comparisons are performed by two-tail Mann-Whitney test. **** $p<0.0001$.

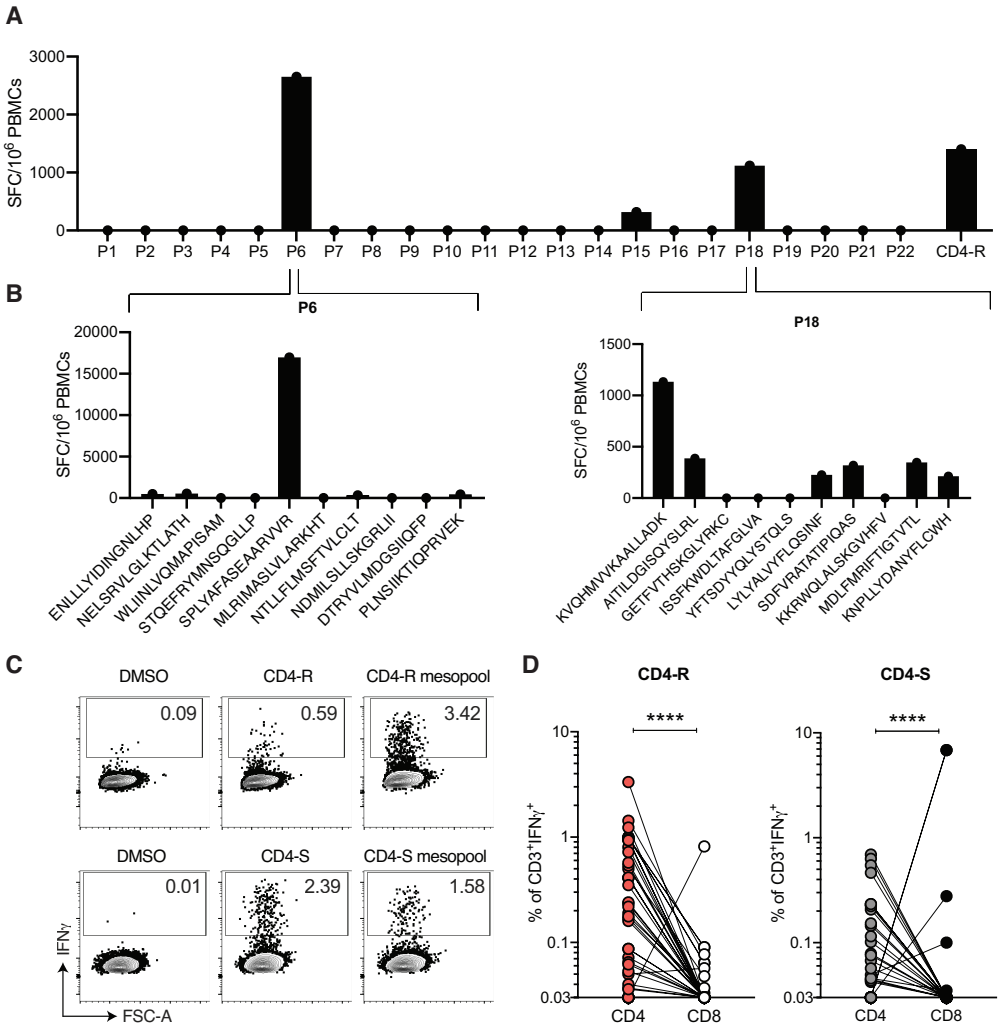

Figure S2: Strategy for SARS-CoV-2-specific epitope identification.

PBMCs from SARS-CoV-2 unexposed donors were stimulated with the CD4-R and CD4-S MPs [1µg/mL] with the addition of IL-2 on day 3, 7, and 11. After 14 days, antigen-specific reactivity against mesopools was assayed by FluoroSPOT. Positive mesopools were deconvoluted 3 days later, by testing for reactivity against the individual peptides contained in the MP. (A-B) SFC/10^6 PBMC for one representative donor for the mesopools (A) and subsequent individual peptide deconvolutions (B). (C) Example of flow cytometry gating strategy for IFNγ detection on T cells at day 17 after stimulation with positive mesopools, negative control (DMSO) or MPs used for *in vitro* stimulation (CD4-R or S). (D) Fraction of antigen-specific response of $CD4^+$ and $CD8^+$ T cells producing $IFN\gamma^+$ after *in vitro* stimulation with CD4-R or CD4R-S. Statistical pairwise comparisons were performed with the Wilcoxon test. **** $p<0.0001$.

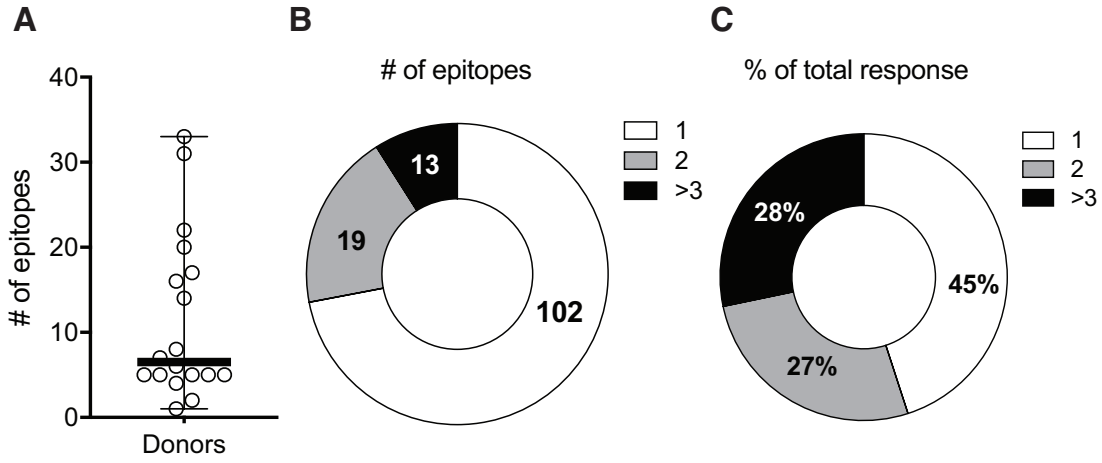

Figure S3: Patterns of epitope recognition in the unexposed donor cohort utilized for epitope identification.

(A) The number of epitopes recognized by each donor are shown. (B-C) The numbers of epitopes and the % of the total response identified in one (white), two (grey) or more than three (black) donors are shown.

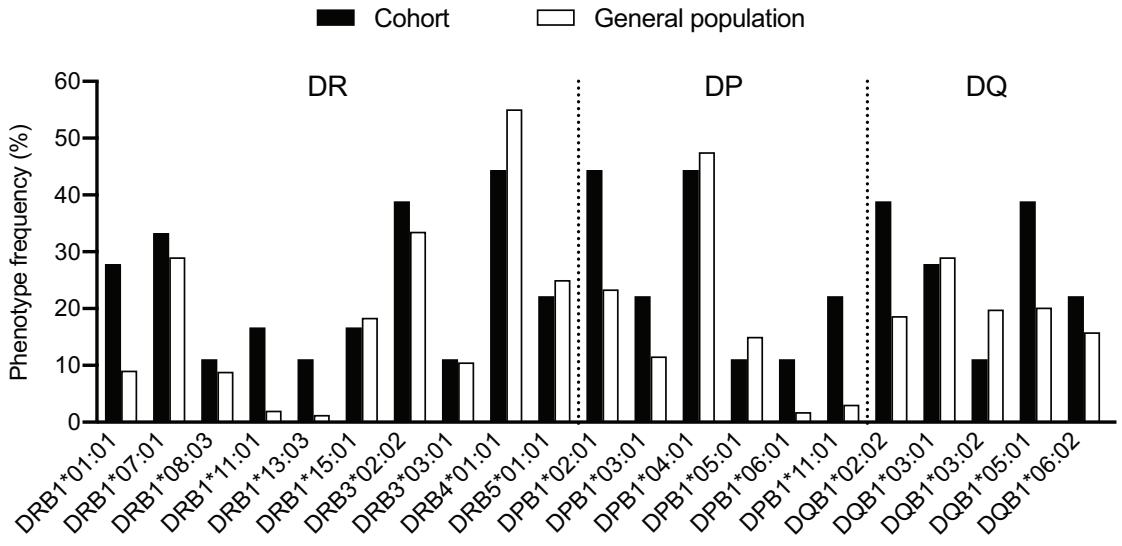

Figure S4. Frequency of common HLA alleles in the unexposed cohort (n= 18) compared to frequencies in a general population cohort (n=3,500).

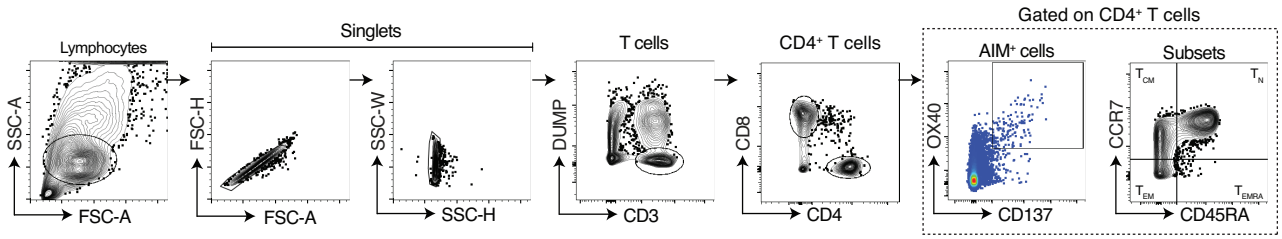

Figure S5: Gating strategy and representative FACS dot plots to determine the T cell memory phenotype.

Example of flow cytometry gating strategy for $CD4^+$ T cells selection. Antigen-specific $CD4^+$ T cells were analyzed based on AIM^+ ($OX40^+$ and $CD137^+$ double expression) after stimulation of PBMCs with HCoV or SARS-CoV-2 peptides. Phenotypes of antigen-specific $CD4^+$ T cells were defined based on the differential expression of CD45RA and CCR7. T cell subsets were defined as naïve (T_N) cells ($CD45RA^+CCR7^+$), central memory (T_{CM}) cells ($CD45RA^-CCR7^+$), effector memory (T_{EM}) cells ($CD45RA^-CCR7^-$), and T_{EM} expressing CD45RA (T_{EMRA}) cells ($CD45RA^+CCR7^-$).

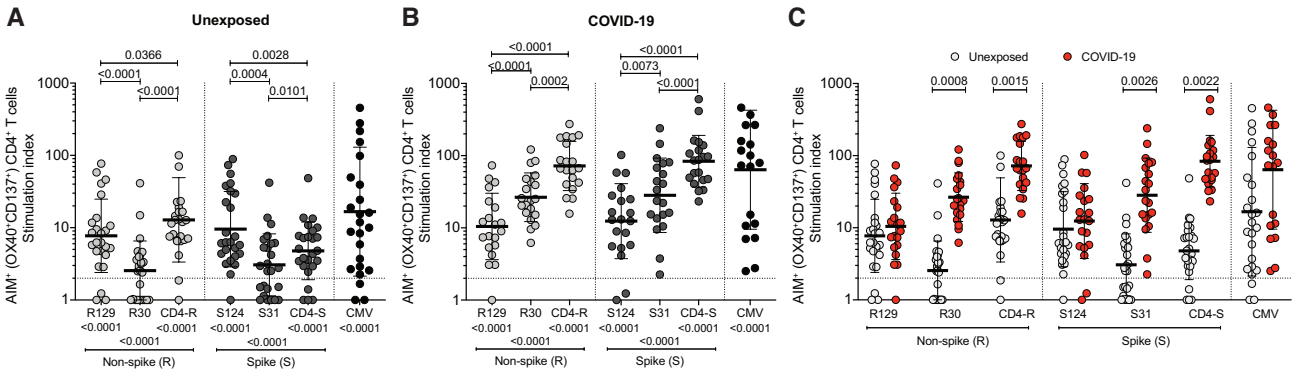

Figure S6: Stimulation index of antigen-specific CD4$^+$ T cell responses against HCoV epitopes homologous to SARS-CoV-2 epitopes.

(A-C) Antigen-specific response quantified by stimulation index (SI) in unexposed and COVID-19 donors. SI was calculated by dividing the percentage of AIM$^+$ cells after pools stimulation with the percentage of AIM$^+$ cells derived from DMSO stimulation. If the AIM$^+$ cells percentage after DMSO stimulation was below the limit of detection, the minimum value across each cohort was used. Statistical pairwise comparisons (A and B) were performed with the Wilcoxon test. (C) Statistical comparisons across cohorts were performed with the Mann-Whitney test. Bottom values represent the p values for overall significance compared to DMSO, calculated by testing the H0 hypothesis of the SI being different from the hypothetical value of 1.0 (Wilcoxon test).

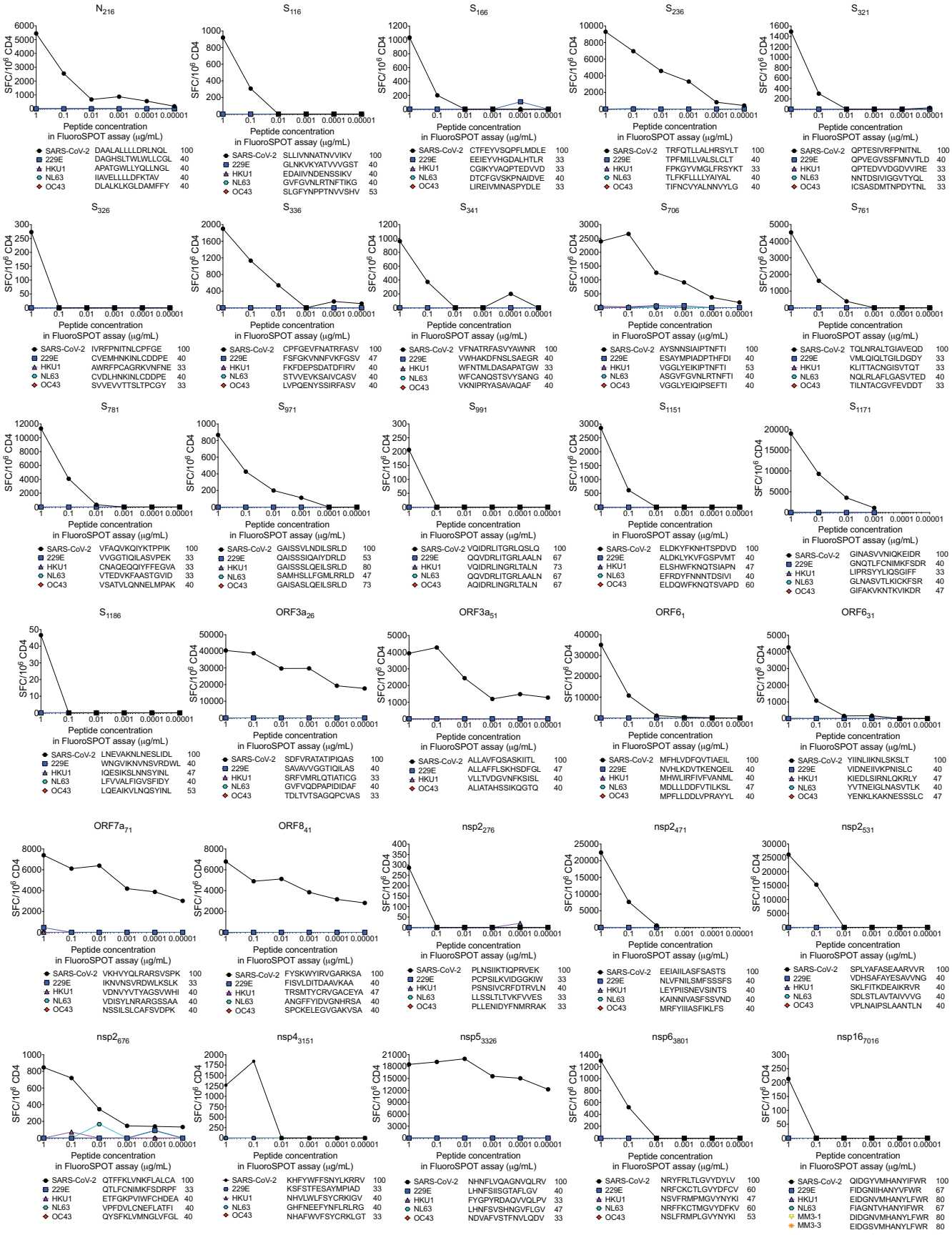
N216
SFC/10^6 CD4
Peptide concentration in FluoroSPOT assay (µg/mL)
SARS-CoV-2 DAALALLLLDRLNQL 100
229E DAGHSLTWLWLLCGL 40
HKU1 APATGWLLYQLLNGL 40
NL63 IIAVELLLLDFKTAV 40
OC43 DLALKLKGLDAMFFY 40
S116
SARS-CoV-2 SLLIVNNATNVVIKV 100
229E GLNKVKYATVVVGST 40
HKU1 EDAIIVNDENSSIKV 40
NL63 GVFGVNLRTNFTIKG 40
OC43 SLGFYNPPTNVVSHV 53
S166
SARS-CoV-2 CTFEYVSQPFLMDLE 100
229E EEIEYVHGDALHTLR 33
HKU1 CGIKYVAQPTEDVVD 33
NL63 DTCFGVSKPNAIDVE 40
OC43 LIREIVMNASPYDLE 33
S236
SARS-CoV-2 TRFQTLLALHRSYLT 100
229E TPFMILLVALSLCLT 40
HKU1 FPKGYVMGLFRSYKT 33
NL63 TLFKFLLLLYAIYAL 40
OC43 TIFNCVYALNNVYLG 40
S321
SARS-CoV-2 QPTESIVRFPNITNL 100
229E QPVEGVSSFMNVTLD 40
HKU1 QPTEDVVDGDVVIRE 33
NL63 NNTDSIVIGGVTYQL 33
OC43 ICSASDMTNPDYTNL 33
S326
SARS-CoV-2 IVRFPNITNLCPFGE 100
229E CVEMHNKINLCDDPE 40
HKU1 AWRFPCAGRKVNFNE 33
NL63 CVDLHNKINLCDDPE 40
OC43 SVVEVVTTSLTPCGY 33
S336
SARS-CoV-2 CPFGEVFNATRFASV 100
229E FSFGKVNNFVKFGSV 47
HKU1 FKFDEPSDATDFIRV 40
NL63 STVVEVKSAIVCASV 40
OC43 LVPQENYSSIRFASV 40
S341
SARS-CoV-2 VFNATRFASVYAWNR 100
229E VWHAKDFNSLSAEGR 40
HKU1 WFNTMLDASAPATGW 33
NL63 WFCANQSTSVYSANG 40
OC43 VKNIPRYASAVAQAF 40
S706
SARS-CoV-2 AYSNNSIAIPTNFTI 100
229E ESAYMPIADPTHFDI 40
HKU1 VGGLYEIKIPTNFTI 53
NL63 ASGVFGVNLRTNFTI 40
OC43 VGGLYEIQIPSEFTI 40
S761
SARS-CoV-2 TQLNRALTGIAVEQD 100
229E VMLQIQLTGILDGDY 33
HKU1 KLITTACNGISVTQT 33
NL63 NQLRLAFLGASVTED 40
OC43 TILNTACGVFEVDDT 33
S781
SARS-CoV-2 VFAQVKQIYKTPPIK 100
229E VVGGTIQILASVPEK 33
HKU1 CNAQEQQIYFFEGVA 33
NL63 VTEDVKFAASTGVID 33
OC43 VSATVLQNNELMPAK 40
S971
SARS-CoV-2 GAISSVLNDILSRLD 100
229E QAISSSIQAIYDRLD 53
HKU1 GAISSSLQEILSRLD 80
NL63 SAMHSLLFGMLRRLD 47
OC43 GAISASLQEILSRLD 73
S991
SARS-CoV-2 VQIDRLITGRLQSLQ 100
229E QQVDRLITGRLAALN 67
HKU1 VQIDRLINGRLTALN 73
NL63 QQVDRLITGRLAALN 67
OC43 AQIDRLINGRLTALN 67
S1151
SARS-CoV-2 ELDKYFKNHTSPDVD 100
229E ALDKLYKVFGSPVMT 40
HKU1 ELSHWFKNQTSIAPN 47
NL63 EFRDYFNNNTDSIVI 40
OC43 ELDQWFKNQTSVAPD 60
S1171
SARS-CoV-2 GINASVVNIQKEIDR 100
229E GNQTLFCNIMKFSDR 40
HKU1 LIPRSYYLIQSGIFF 33
NL63 GLNASVTLKICKFSR 40
OC43 GIFAKVKNTKVIKDR 47
S1186
SARS-CoV-2 LNEVAKNLNESLIDL 100
229E WNGVIKNVNSVRDWL 40
HKU1 IQESIKSLNNSYINL 47
NL63 LFVVALFIGVSFIDY 40
OC43 LQEAIKVLNQSYINL 53
ORF3a26
SARS-CoV-2 SDFVRATATIPIQAS 100
229E SAVAVVGGTIQILAS 40
HKU1 SRFVMRLQTIATICG 33
NL63 GVFVQDPAPIDIDAF 40
OC43 TDLTVTSAGQPCVAS 33
ORF3a51
SARS-CoV-2 ALLAVFQSASKIITL 100
229E ALLAFFLSKHSDFGL 47
HKU1 VLLTVDGVNFKSISL 40
OC43 ALIATAHSSIKQGTQ 40
ORF61
SARS-CoV-2 MFHLVDFQVTIAEIL 100
229E NVHLKDVTKENQEIL 40
HKU1 MHWLIRFIVFVANML 40
NL63 MDLLLLDDFVTILKSL 47
OC43 MPFLLDDLVPRAYYL 40
ORF631
SARS-CoV-2 YIINLIIKNLSKSLT 100
229E VIDNEIIVKPNISLC 40
HKU1 KIEDLSIRNLQKRLY 47
NL63 YVTNEIGLNASVTLK 40
OC43 YENKLKAKNESSSLC 47
ORF7a71
SARS-CoV-2 VKHVYQLRARSVSPK 100
229E IKNVNSVRDWLKSLK 33
HKU1 VDNVYVTYAGSVWHI 40
NL63 VDISYLNRARGSSAA 40
OC43 NSSILSLCAFSVDPK 40
ORF841
SARS-CoV-2 FYSKWYIRVGARKSA 100
229E FISVLDITDAAVKAA 40
HKU1 TRSMTYCRVGACEYA 47
NL63 ANGFFYIDVGNHRSA 40
OC43 SPCKELEGVGAKVSA 40
nsp2276
SARS-CoV-2 PLNSIIKTIQPRVEK 100
229E PCPSILKVIDGGKIW 33
HKU1 PSNSIVCRFDTRVLN 40
NL63 LLSSLTLTVKFVVES 33
OC43 PLLENIDYFNMRRAK 33
nsp2471
SARS-CoV-2 EEIAIILASFSASTS 100
229E NLVFNILSMFSSSFS 40
HKU1 LEYPIISNEVSINTS 40
NL63 KAINNIVASFSSSVND 40
OC43 MRFYIIIASFIKLFS 40
nsp2531
SARS-CoV-2 SPLYAFASEAARVVR 100
229E VDHSAFAYESAVVNG 40
HKU1 SKLFITKDEAIKRVR 40
NL63 SDLSTLAVTAIVVVG 40
OC43 VPLNAIPSLAANTLN 40
nsp2676
SARS-CoV-2 QTFFKLVNKFLALCA 100
229E QTLFCNIMKFSDRPF 33
HKU1 ETFGKPVIWFCHDEA 40
NL63 VPFDVLCNEFLATFI 40
OC43 QYSFKLVMNGLVFGL 40
nsp43151
SARS-CoV-2 KHFYWFFSNYLKRRV 100
229E KSFSTFESAYMPIAD 33
HKU1 NHVLWLFSYCRKIGV 40
NL63 GHFNEEFYNFLRLRG 40
OC43 NHAFWVFSYCRKLGT 33
nsp53326
SARS-CoV-2 NHNFLVQAGNVQLRV 100
229E LHNFSIISGTAFLGV 40
HKU1 FYGPYRDAQVVQLPV 33
NL63 LHNFSVSHNGVFLGV 47
OC43 NDVAFVSTFNVLQDV 33
nsp63801
SARS-CoV-2 NRYFRLTLGVYDYLV 100
229E NRFCKCTLGVYDFCV 60
HKU1 NSVFRMPMGVYNYKI 47
NL63 NRFFKCTMGVYDFKV 60
OC43 NSLFRMPLGVYNYKI 53
nsp167016
SARS-CoV-2 QIDGYVMHANYIFWR 100
229E FIDGNIIHANYVFWR 67
HKU1 EIDGNVMHANYLFWR 80
NL63 FIAGNTVHANYIFWR 67
MM3-1 DIDGNVMHANYLFWR 80
MM3-3 EIDGSVMHANYLFWR 80

Figure S7: Non-cross-reactive SARS-CoV-2 T cell epitopes.
Short-term cell lines (30) generated using specific SARS-CoV-2 epitope/donor combinations selected on the basis of the primary screen. After a 14 days *in vitro* expansion, each TCL was tested with the SARS-CoV-2 epitope used for stimulation and peptides corresponding to analogous sequences from other HCoV at six different concentrations (1 μg/mL, 0.1 μg/mL, 0.01 μg/mL, 0.001 μg/mL, 0.0001 μg/mL, and 0.00001 μg/mL). Spot Forming Cells per million (SFC/10^6) PBMCs are plotted for TCLs stimulated with each peptide.

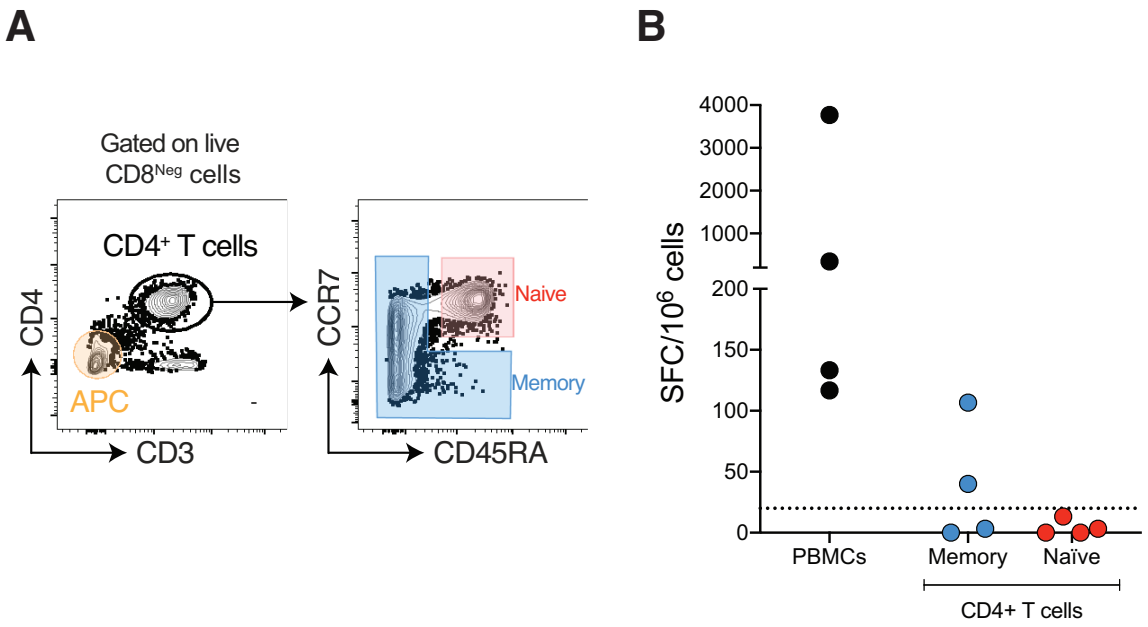

Figure S8: T cells responding to the CD4-[S31] epitope pool are derived from the memory compartment.

(A) Example of flow cytometry gating strategy for sorting naïve ($CD45RA^+$ $CCR7^+$, red gate) and memory $CD4^+$ T cells ($CD45RA^-$ $CCR7^{+/-}$, blue gate). CD3- cells (orange gate) were utilized as antigen presenting cells. (B) Response of PBMCs and memory or naïve $CD4^+$ T cells cocultured with APCs (1:2 ratio) after 14 days *in vitro* expansion with and tested against the CD4-[S31] epitope pool. Spot Forming Cells per million ($SFC/10^6$) cells are plotted for each T cell lines stimulated with each peptide. The dotted line at 20 $SFC/10^6$ represents the cut-off for positivity in this assay.

Supplemental tables

Table S1: All epitopes identified in this study

Sequence	Protein	Start	"+"/ tested	SFC (10^6 PBMC)	Response type	Potential HLA restriction(s)	CD4R -30	CD4 S-31
NHNFLVQAGNVQLRV	nsp5	3326	2/16	51907	CD4	DRB1*0101, *0701, *0803, *1501, DQA1*0501/DQB1*0301, *0102/*0602	Yes	No
SFIEDLLFNKVTLAD	S (non-RBD)	816	7/15	30487	CD4	DRB1*0101, *0103, *0404, *1102, *1303, *1401, *1501, *1602, DQA1*0101/DQB1*0501, *0102/*0502	No	Yes
SPLYAFASEAARVVR	nsp2	531	1/17	15860	CD4	DRB1*0701, DQA1*0201/DQB1*0202	Yes	No
SDFVRATATIPIQAS	ORF3a	26	1/17	14667	CD4	DRB1*0701, DQA1*0201/DQB1*0202	Yes	No
QPTESIVRFPNITNL	S (RBD)	321	5/16	14033	CD4/ undetermined	DRB1*0803, *1501	No	Yes
FYSKWYIRVGARKSA	ORF8	41	1/15	12400	CD4	DRB1*0101, *0701	Yes	No
TRFQTLLALHRSYLT	S (non-RBD)	236	5/13	11813	CD4/ undetermined	DRB1*0101, *0701, *0803, *1102, *1301, *1302, *1303, *1501, DQA1*0101/DQB1*0501, *0102/*0602, *0103/*0603	No	Yes
SNFRVQPTESIVRFP	S (RBD)	316	1/16	11693	CD4	DRB1*0301	No	Yes
EEIAIILASFSASTS	nsp2	471	1/16	11680	CD4	DRB1*0410, *0701, DQA1*0201/DQB1*0202, *0301/*0302	Yes	No
MFHLVDFQVTIAEIL	ORF6	1	1/16	10817	CD4	DRB1*1303	Yes	No
KPSKRSFIEDLLFNK	S (non-RBD)	811	4/15	10793	CD4	DRB1*0301, DQA1*0501/DQB1*0201, *0201/*0202, *0101/*0501	No	Yes
TQLNRALTGIAVEQD	S (non-RBD)	761	3/14	10193	CD4	DRB1*0101, *0901, DQA1*0301/DQB1*0303, *0301/*0402, *0102/*0602, *0102/*0604	No	Yes
NFSQILPDPSKPSKR	S (non-RBD)	801	1/15	10160	CD4		No	Yes
NNATNVVIKVCEFQF	S (non-RBD)	121	3/16	9760	CD4		No	Yes
AQALNTLVKQLSSNF	S (non-RBD)	956	2/14	7300	CD4	DRB1*1101, *1303, DQA1*0102/DQB1*0602	No	Yes

IVRFPNITNLCPFGE	S (RBD)	326	2/16	7227	CD4		No	Yes
VLKKLKKSLNVAKSE	nsp8	3976	1/16	5660	CD4	DRB1*0803, *1202	Yes	No
LNEVAKNLNESLIDL	S (non-RBD)	1186	1/17	5213	CD4	DRB1*1302	No	Yes
CTFEYVSQPFLMDLE	S (non-RBD)	166	3/15	4753	CD4	DQA1*0102/DQB1*0604	No	Yes
ISPYNSQNAVASKIL	nsp13	5836	2/18	4440	CD4	DRB1*0101, DQA1*0102/DQB1*0602	Yes	No
NRYFRLTLGVYDYLV	nsp6	3801	4/16	4253	CD4	DRB1*0101, *0103, *0701, *0803, *1501, DQA1*0201/DQB1*0202, *0101/*0501, *0102/*0602	Yes	No
NLLLQYGSFCTQLNR	S (non-RBD)	751	1/14	3933	CD4	DRB1*0101, *1501, DQA1*0101/DQB1*0501	No	Yes
LMIERFVSLAIDAYP	nsp12	5246	2/17	3870	CD4	DRB1*0103, *0701, *0803, *1202, DQA1*0201/DQB1*0202, *0501/*0301, *0101/*0501, *0103/*0601	Yes	No
DAALALLLLDRLNQL	N	216	1/15	3733	CD4	DRB1*1101, DQA1*0101/DQB1*0501	Yes	No
SVASQSIIAYTMSLG	S (non-RBD)	686	2/15	3360	CD8		No	Yes
SLLIVNNATNVVIKV	S (non-RBD)	116	1/16	3327	CD4	DRB1*0701, *1301, DQA1*0103/DQB1*0603	No	Yes
VKHVYQLRARSVSPK	ORF7a	71	1/16	3307	CD4	DRB1*0103, *0701	Yes	No
VQIDRLITGRLQSLQ	S (non-RBD)	991	3/14	3007	CD4	DRB1*0101, *0301, *1101, *1303	No	Yes
VFNATRFASVYAWNR	S (RBD)	341	4/16	2540	CD4/ undetermined	DRB1*0101, *0803, *1101, *1303, *1501, DQA1*0501/DQB1*0301, *0102/*0602	No	Yes
PLNSIIKTIQPRVEK	nsp2	276	2/17	2520	CD4	DRB1*0101, *0701	Yes	No
APHGVVFLHVTYVPA	S (non-RBD)	1056	1/14	2433	CD4	DRB1*0404, *1001, DQA1*0101/DQB1*0501	No	Yes
TFKVSIWNLDYIINL	ORF6	21	2/16	2427	CD4	DRB1*0103, *0701, *1501, DQA1*0201/DQB1*0202, *0101/*0501	Yes	No
KVTFFPDLNGDVVAI	nsp3	1956	1/16	2427	CD4	DQA1*0201/DQB1*0202, *0101/*0501	Yes	No
AQYTSALLAGTITSG	S (non-RBD)	871	1/12	2400	CD4		No	Yes
CPFGEVFNATRFASV	S (RBD)	336	3/16	2360	CD4/ undetermined	DRB1*0101, *0803, *1101, *1102, *1303, DQA1*0501/DQB1*0301, *0102/*0602	No	Yes
ELDKYFKNHTSPDVD	S (non-RBD)	1151	2/16	2313	CD4		No	Yes
FTVEKGIYQTSNFRV	S (non-RBD)	306	1/16	2053	CD4		No	Yes

CEFQFCNDPFLGVYY	S (non-RBD)	131	2/16	2000	CD4	DQA1*0201/DQB1*0202, *0101/*0501	No	Yes
LAILTALRLCAYCCN	E	31	1/17	1880	CD4	DRB1*0101, *1101	Yes	No
VFAQVKQIYKTPPIK	S (non-RBD)	781	1/14	1673	CD4		No	Yes
LLALHRSYLTPGDSS	S (non-RBD)	241	3/13	1613	CD4	DRB1*0101, *0701, *1102, *1501	No	No
IGINITRFQTLLALH	S (non-RBD)	231	2/13	1593	CD4/ undetermined	DRB1*0701, *1102, *1301, *1303, DQA1*0103/DQB1*0603	No	Yes
AYSNNSIAIPTNFTI	S (non-RBD)	706	1/15	1587	CD4	DQA1*0103/DQB1*0603	No	Yes
KHFYWFFSNYLKRRV	nsp4	3151	2/17	1573	CD4	DRB1*0410, *0701, *0901, DQA1*0201/DQB1*0202, *0301/*0402	Yes	No
GINASVVNIQKEIDR	S (non-RBD)	1171	1/17	1547	CD4	DQA1*0501/DQB1*0301	No	Yes
SIIAYTMSLGAENSV	S (non-RBD)	691	3/15	1427	CD4 and CD8	DRB1*0103, *0701, DQA1*0201/DQB1*0202, *0101/*0501	No	No
YIINLIIKNLSKSLT	ORF6	31	1/16	1343	CD4	DRB1*1102, *1303	Yes	No
GETFVTHSKGLYRKC	nsp2	706	1/17	1333	CD4	DRB1*0701	No	No
REEAIRHVRAWIGFD	nsp14	6001	2/16	1267	CD4	DRB1*0103, *0701	Yes	No
WTFGAGAALQIPFAM	S (non-RBD)	886	1/12	1253	CD4	DRB1*0101, DQA1*0501/DQB1*0301	No	Yes
TQLCQYLNTLTLAVP	nsp16	6846	1/17	1187	CD4	DRB1*0101, *1501, DQA1*0101/DQB1*0501, *0102/*0602	Yes	No
ALLAVFQSASKIITL	ORF3a	51	1/17	1160	CD4	DRB1*0701, *1301, DQA1*0103/DQB1*0603	Yes	No
LLLLDRLNQLESKMS	N	221	1/15	1120	CD4	DRB1*1101, DQA1*0101/DQB1*0501	Yes	No
GAISSVLNDILSRLD	S (non-RBD)	971	1/14	1120	CD4	DQA1*0101/DQB1*0501	No	Yes
PSGTWLTYTGAIKLD	N	326	1/15	1067	CD4	DRB1*0103, *0701	Yes	No
GLVASIKNFKSVLYY	nsp12	5166	1/16	1060	CD4	DRB1*0803, *1202, DQA1*0103/DQB1*0601	No	No
QTFFKLVNKFLALCA	nsp2	676	1/17	1053	CD4	DRB1*0103, *0701, DQA1*0101/DQB1*0501	Yes	No
SHNIALIWNVKDFMS	nsp3	2706	2/14	1040	CD4	DRB1*0410, DQA1*0201/DQB1*0202, *0301/*0302, *0301/*0402	No	No
QNCVLKLKVDTANPK	nsp5	3346	2/17	1000	CD4	DRB1*0410	No	No
FGEYSHVVAFNTLLF	nsp4	3071	1/17	893	CD4	DRB1*0410,*0701, DQA1*0201/DQB1*0202, *0301/*0302	No	No
SIAIPTNFTISVTTE	S (non-RBD)	711	2/15	880	CD4	DQA1*0201/DQB1*0202,*0102/*0602	No	No
LPQGFSALEPLVDLP	S (non-RBD)	216	1/13	873	CD4		No	No

LFVAAIFYLITPVHV	nsp4	2781	2/16	840	CD4	DRB1*0103, *0701, DQA1*0201/DQB1*0202, *0101/*0501	No	No
FNFNGLTGTGVLTES	S (non-RBD)	541	1/13	840	CD4	DRB1*0101, DQA1*0102/DQB1*0602	No	No
LEASFNYLKSPNFSK	nsp3	2211	1/17	840	CD4	DRB1*0410, *0701	No	No
LIVTALRANSAVKLQ	nsp8	4126	1/17	813	CD4	DRB1*0701, *1301, DQA1*0103/DQB1*0603	No	No
GSLIYSTAALGVLMS	nsp3	2241	1/17	800	CD4	DRB1*0101, *1101, DQA1*0501/DQB1*0301	No	No
EFYAYLRKHFSMMIL	nsp12	5136	2/18	787	CD4	DRB1*0701, *0901, *1301, DQA1*0301/DQB1*0402	Yes	No
IWNLDYIINLIIKNL	ORF6	26	1/16	787	CD4	DRB1*0101, *1501, DQA1*0101/DQB1*0501	No	No
GGNYNYLYRLFRKSN	S (RBD)	446	1/16	787	CD4	DRB1*1102, *1303	No	No
NVNRFNVAITRAKVG	nsp13	5881	1/18	760	CD4	DRB1*0803, *1501, DQA1*0501/DQB1*0301, *0102/*0602	Yes	No
KKRWQLALSKGVHFV	ORF3a	66	2/17	760	CD4	DRB1*0701, *0901, DQA1*0301/DQB1*0402	No	No
LITGRLQSLQTYVTQ	S (non-RBD)	996	2/14	760	CD4	DRB1*0101, *1501, DQA1*0102/DQB1*0602	No	No
LIIMRTFKVSIWNLD	ORF6	16	1/16	733	CD4	DRB1*0101, *1101, DQA1*0101/DQB1*0501	No	No
TDEMIAQYTSALLAG	S (non-RBD)	866	1/12	720	CD4	DRB1*0410, *0701, DQA1*0201/DQB1*0202, *0301/*0302	No	No
HWFVTQRNFYEPQII	S (non-RBD)	1101	1/13	707	CD4	DQA1*0101/DQB1*0501	No	No
YIRVGARKSAPLIEL	ORF8	46	2/15	673	CD4	DRB1*0101, *0103, *0701	No	No
QIDGYVMHANYIFWR	nsp16	7016	1/14	667	CD8		Yes	No
NMFITREEAIRHVRA	nsp14	5996	1/16	667	CD4	DRB1*0101, *1101	No	No
TIAYIICISTKHFYW	nsp4	3141	1/17	667	Undetermined	DRB1*0103, *0701	No	No
DDQIGYYRRATRRIR	N	81	1/15	653	CD4	DRB1*0103, *0701	No	No
FNCYFPLQSYGFQPT	S (RBD)	486	1/16	647	CD4	DRB1*0101, DQA1*0101/DQB1*0501	No	No
CAQKFNGLTVLPPLL	S (non-RBD)	851	1/12	640	CD4	DRB1*0101, *1501, DQA1*0101/DQB1*0501, *0102/*0602	No	Yes
STECSNLLLQYGSFC	S (non-RBD)	746	2/15	633	CD4		No	No
RFASVYAWNRKRISN	S (RBD)	346	1/16	627	Undetermined	DRB1*1102, *1303	No	No
NIDGYFKIYSKHTPI	S (non-RBD)	196	1/15	607	CD4	DRB1*1501	No	No
AENSVAYSNNSIAIP	S (non-RBD)	701	1/15	540	CD4	DRB1*0803, DQA1*0501/DQB1*0301, *0102/*0602	No	No
EIIKSQDLSVVSKVV	nsp15	6756	1/18	533	CD4	DRB1*0404	No	No

CTFLLNKEMYLKLRS	nsp4	3181	1/17	520	CD4	DRB1*0101, *1101, DQA1*0101/DQB1*0501	No	No
YGSFCTQLNRALTGI	S (non-RBD)	756	1/14	507	CD4	DRB1*0901, DQA1*0301/DQB1*0303, *0301/*0402	No	No
NELSRVLGLKTLATH	nsp3	2111	1/17	493	CD4	DRB1*0701	No	No
DAFKLNIKLLGVGGK	nsp6	3836	1/16	480	CD4	DRB1*0101, *1101	No	No
IPFAMQMAYRFNGIG	S (non-RBD)	896	1/12	480	CD4	DRB1*0101, *1101, DQA1*0101/DQB1*0501	No	No
FLGIITTVAAFHQEC	ORF8	6	1/15	480	CD4	DRB1*0103, *0701, DQA1*0201/DQB1*0202	No	No
GIYQTSNFRVQPTES	S (RBD)	311	2/16	467	CD4/ undetermined	DRB1*0101, *1303	No	No
ENLLLYIDINGNLHP	nsp3	1251	1/17	453	CD4		No	No
LYSPIFLIVAAIVFI	ORF7a	96	1/16	453	CD4		No	No
LGDISGINASVVNIQ	S (non-RBD)	1166	1/17	453	CD4	DQA1*0501/DQB1*0301	No	No
VLLPLVSSQCVNLTT	S (non-RBD)	6	1/16	440	CD4	DRB1*0701	No	No
VLSFCAFAVDAAKAY	nsp10	4266	2/16	440	CD4	DRB1*0103, *0701, DQA1*0201/DQB1*0202, *0101/*0501	No	No
LLVLVQSTQWSLFFF	nsp6	3591	1/16	400	CD4	DRB1*0701, DQA1*0201/DQB1*0202	No	No
QSINFVRIIMRLWLC	ORF3a	116	1/17	400	CD4	DRB1*0701, *1301	No	No
KNPLLYDANYFLCWH	ORF3a	136	1/17	400	CD4	DQA1*0201/DQB1*0202	No	No
QPYVFIKRSDARTAP	nsp1	66	1/14	387	CD8		No	No
TNFTISVTTEILPVS	S (non-RBD)	716	2/15	387	CD4	DRB1*0101, *0103, *0701, DQA1*0201/DQB1*0202, *0501/*0301	No	No
FDAYVNTFSSTFNVP	nsp3	2591	1/17	373	Undetermined	DRB1*0701, DQA1*0201/DQB1*0202	No	No
LRKHFSMMILSDDAV	nsp12	5141	1/18	360	CD4	DRB1*0103, *1102, *1303	Yes	No
GCVIAWNSNNLDSKV	S (RBD)	431	1/16	360	CD4	DRB1*0701, *1301, DQA1*0201/DQB1*0202, *0103/*0603	No	No
SEETGTLIVNSVLLF	E	6	1/17	360	CD4	DQA1*0501/DQB1*0301	No	No
LGVYYHKNNKSWMES	S (non-RBD)	141	2/16	360	CD4	DRB1*1303	No	No
IAEILLIIMRTFKVS	ORF6	11	1/16	347	CD4	DRB1*0103, *0701	No	No
DNFKFVCDNIKFADD	nsp3	1926	1/17	333	Undetermined	DQA1*0101/DQB1*0501	No	No
QMAYRFNGIGVTQNV	S (non-RBD)	901	2/15	333	CD4	DRB1*0101, *0701, DQA1*0501/DQB1*0301, *0103/*0603	No	No
SLLMPILTLTRALTA	nsp12	4631	1/17	320	CD4	DRB1*0803, *1501, DQA1*0102/DQB1*0602	No	No
MKIILFLALITLATC	ORF7a	1	1/16	320	CD4		No	No
KGGKIVNNWLKQLIK	nsp4	2761	1/18	307	CD4	DRB1*1301	No	No

VVIKVCEFQFCNDPF	S (non-RBD)	126	1/16	307	CD4	DQA1*0101/DQB1*0501	No	No
ECDIPIGAGICASYQ	S (non-RBD)	661	1/15	307	CD4		No	No
NTLLFLMSFTVLCLT	nsp4	3081	1/17	307	CD4		No	No
ISSFKWDLTAFGLVA	nsp3	2311	1/17	293	CD4	DRB1*0701, DQA1*0201/DQB1*0202	No	No
PDILRVYANLGERVR	nsp12	4561	1/16	267	CD4	DRB1*0803, *1202, DQA1*0103/DQB1*0601	No	No
PLMYKGLPWNVVRIK	nsp14	6076	1/16	260	CD4	DRB1*0803, *1202, DQA1*0501/DQB1*0301, *0103/*0601	No	No
EAARYMRSLKVPATV	nsp3	1461	1/16	253	CD4	DRB1*0701	No	No
SLFFFLYENAFLPFA	nsp6	3601	1/18	240	CD4	DRB1*0101, *1501, DQA1*0101/DQB1*0501	No	No
SVLHSTQDLFLPFFS	S (non-RBD)	46	1/16	227	CD4	DQA1*0101/DQB1*0501	No	No
AITILDGISQYSLRL	nsp2	566	1/17	227	CD4		No	No
DTRYVLMDGSIIQFP	nsp4	2951	1/17	213	CD4	DRB1*0404, *1001, DQA1*0301/DQB1*0302, *0101/*0501	No	No
LVYFLQSINFVRIIM	ORF3a	111	1/17	200	CD4	DRB1*0701, *1301, DQA1*0103/DQB1*0603	No	No
YEQYIKWPWYIWLGF	S (non-RBD)	1206	1/17	200	CD4		No	Yes
REGVFVSNGTHWFVT	S (non-RBD)	1091	1/14	187	CD4	DRB1*0103, *0701	No	No
TTAPAICHDGKAHFP	S (non-RBD)	1076	1/14	187	CD4		No	No
KLLKSIAATRGATVV	nsp12	4966	1/17	187	CD4	DRB1*0404, *1001	Yes	No
TSHKLVLSVNPYVCN	nsp13	5361	1/17	160	CD4	DRB1*0701, *1301, DQA1*0103/DQB1*0603	Yes	No
SFTRGVYYPDKVFRS	S (non-RBD)	31	1/16	160	CD4		No	No
CTLKSFTVEKGIYQT	S (non-RBD)	301	1/16	147	CD4	DRB1*1501	No	No
LCLFLLPSLATVAYF	nsp6	3636	1/18	120	CD4	DRB1*0101, *1501, DQA1*0101/DQB1*0501, *0102/*0602	No	No
TLVYKVYYGNALDQA	nsp6	3716	1/17	120	CD4	DRB1*0101, *1501, DQA1*0101/DQB1*0501	No	No
LLFNKVTLADAGFIK	S (non-RBD)	821	1/15	107	CD4	DRB1*0101, DQA1*0501/DQB1*0301	No	No
KAHFPREGVFVSNGT	S (non-RBD)	1086	1/14	107	CD4		No	No
TLVKQLSSNFGAISS	S (non-RBD)	961	1/14	93	CD4	DRB1*0101, *1101, DQA1*0501/DQB1*0301	No	No
GKIADYNYKLPDDFT	S (RBD)	416	1/16	80	CD4		No	No
YNYKLPDDFTGCVIA	S (RBD)	421	1/16	53	CD4		No	No

Table S2: Composition of the Human Coronavirus homologs of SARS-CoV-2 CD4R epitopes (HCoV-R129

Sort	Sequence	Organism	Protein	Start
1	NRYFRLTLGVYDYLV	SARS-CoV-2	nsp6	3801
2	NRFCKCTLGVYDFCV	229E		
3	NSVFRMPMGVYNYKI	HKU1		
4	NRFFKCTMGVYDFKV	NL63		
5	NSLFRMPLGVYNYKI	OC43		
6	KHFYWFFSNYLKRRV	SARS-CoV-2	nsp4	3151
7	KSFSTFESAYMPIAD	229E		
8	NHVLWLFSYCRKIGV	HKU1		
9	GHFNEEFYNFLRLRG	NL63		
10	NHAFWVFSYCRKLGT	OC43		
11	PLNSIIKTIQPRVEK	SARS-CoV-2	nsp2	276
12	PCPSILKVIDGGKIW	229E		
13	PSNSIVCRFDTRVLN	HKU1		
14	LLSSLTLTVKFVVES	NL63		
15	PLLENIDYFNMRRAK	OC43		
16	LMIERFVSLAIDAYP	SARS-CoV-2	nsp12	5246
17	ILLERYVSLAIDAYP	229E		
18	LLIERFVSLAIDAYP	HKU1		
19	VLLERYVSLAIDAYP	NL63		
20	LLIKRFVSLAIHAYP	MM3-2		
21	EFYAYLRKHFSMMIL	SARS-CoV-2	nsp12	5136
22	DFYGYLQKHFSMMIL	229E		
23	EYYEFLCKHFSMMIL	HKU1		
24	DYYGYLRKHFSMMIL	NL63		
25	EYYEFLNKHFSMMIL	OC43		
26	EFYEFLNKHFSMMIL	MM3-2		
27	NHNFLVQAGNVQLRV	SARS-CoV-2	nsp5	3326
28	LHNFSIISGTAFLGV	229E		
29	FYGPYRDAQVVQLPV	HKU1		
30	LHNFSVSHNGVFLGV	NL63		
31	NDVAFVSTFNVLQDV	OC43		
32	REEAIRHVRAWIGFD	SARS-CoV-2	nsp14	6001
33	RDFAMRHVRGWLGMD	229E		
34	KDEAIKRVRGWVGFD	HKU1		
35	RDFAIRNVRGWLGMD	NL63		
36	KEEAVKRVRAWVGFD	OC43		
37	RDEAIRRVRAWVGFD	MM3-1		
38	TFKVSIWNLDYIINL	SARS-CoV-2	ORF6	21
39	NDKITEFQLDYSIDV	229E		
40	LERVSLWNYGKPINL	HKU1		
41	LFTNSILMLDKQGQL	NL63		
42	YQKVFRVYLAYIKKL	OC43		

43	NVNRFNVAITRAKVG	SARS-CoV-2	nsp13	5881
44	NANRFNVAITRAKKG	229E		
45	NVNRFNVAITRAKKG	HKU1		
46	NVNRFNLAITRAKKG	MM3-1		
47	NVNRFNVAITRARKG	MM3-3		
48	LRKHFSMMILSDDAV	SARS-CoV-2	nsp12	5141
49	LQKHFSMMILSDDSV	229E		
50	LCKHFSMMILSDDGV	HKU1		
51	LRKHFSMMILSDDGV	NL63		
52	LNKHFSMMILSDDGV	OC43		
53	FNKHFSMMILSDDGV	MM3-1		
54	LFFHFSMMILSDDGV	MM3-3		
55	LNKHFNMMILSDDGV	MM3-4		
56	LNKHFSMIILSDDGV	MM3-5		
57	SPLYAFASEAARVVR	SARS-CoV-2	nsp2	531
58	VDHSAFAYESAVVNG	229E		
59	SKLFITKDEAIKRVR	HKU1		
60	SDLSTLAVTAIVVVG	NL63		
61	VPLNAIPSLAANTLN	OC43		
62	EEIAIILASFSASTS	SARS-CoV-2	nsp2	471
63	NLVFNILSMFSSSFS	229E		
64	LEYPIISNEVSINTS	HKU1		
65	KAINNIVASFSSVND	NL63		
66	MRFYIIIASFIKLFS	OC43		
67	VLKKLKKSLNVAKSE	SARS-CoV-2	nsp8	3976
68	IIKQLKKAMNVAKAE	229E		
69	QIKQLEKACNIAKSV	HKU1		
70	LIKQLKRAMNIAKSE	NL63		
71	QLKQLEKACNIAKSA	OC43		
72	TQLCQYLNTLTLAVP	SARS-CoV-2	nsp16	6846
73	TQLCQYFNSTTLCVP	229E		
74	TQLCQYLNTTTLAVP	HKU1		
75	TQLCQYLNSTTMCVP	NL63		
76	TQLCQYLNTTTIAVP	MM3-1		
77	TQLCQYLSTTTIAVP	MM3-3		
78	TQLCQYLSTTTLAVP	MM3-4		
79	ISPYNSQNAVASKIL	SARS-CoV-2	nsp13	5836
80	ISPYNSQNYVAARLL	229E		
81	ISPYNSQNYVAKRVL	HKU1		
82	ISPYNSQNYVASRFL	NL63		
83	ISPYNSQNFAAKRVL	OC43		
84	ISPYNSQNYVAKRIL	MM3-1		
85	TSHKLVLSVNPYVCN	SARS-CoV-2	nsp13	5361
86	TDHKFILAITPYVCN	229E		
87	TNHKYVLSVSPYVCN	HKU1		
88	TDHKYVLSVSPYVCN	OC43		

89	TDHKYVLSVAPYVCN	MM3-1		
90	KVTFFPDLNGDVVAI	SARS-CoV-2	nsp3	1956
91	QEATLPDIAEDVVDQ	229E		
92	KVTVWPVATGDVVLA	HKU1		
93	KDGFFTYLNGVIREK	NL63		
94	KITEWPTATGDVVLA	OC43		
95	QTFFKLVNKFLALCA	SARS-CoV-2	nsp2	676
96	QTLFCNIMKFSDRPF	229E		
97	ETFGKPVIWFCHDEA	HKU1		
98	VPFDVLCNEFLATFI	NL63		
99	QYSFKLVMNGLVFGL	OC43		
100	KLLKSIAATRGATVV	SARS-CoV-2	nsp12	4966
101	KCLKSIVATRNATVV	229E		
102	KCLKSIAATRGVPVV	HKU1		
103	KHLKSIVNTRNATVV	NL63		
104	KCLKSIAATRGVSVV	MM3-2		
105	QIDGYVMHANYIFWR	SARS-CoV-2	nsp16	7016
106	FIDGNIIHANYVFWR	229E		
107	EIDGNVMHANYLFWR	HKU1		
108	FIAGNTVHANYIFWR	NL63		
109	DIDGNVMHANYLFWR	MM3-1		
110	EIDGSVMHANYLFWR	MM3-3		
111	SDFVRATATIPIQAS	SARS-CoV-2	ORF3a	26
112	SAVAVVGGTIQILAS	229E		
113	SRFVMRLQTIATICG	HKU1		
114	GVFVQDPAPIDIDAF	NL63		
115	TDLTVTSAGQPCVAS	OC43		
116	ALLAVFQSASKIITL	SARS-CoV-2	ORF3a	51
117	ALLAFFLSKHSDFGL	229E		
118	VLLTVDGVNFKSISL	HKU1		
119	ALIATAHSSIKQGTQ	OC43		
120	LAILTALRLCAYCCN	SARS-CoV-2	E	31
121	LAKFTKLLLLIYTLY	229E		
122	LALLYRNLKCSYVLN	HKU1		
123	STILQAAGLCVVCGS	NL63		
124	LQSAATIRSVAYVAN	OC43		
125	YIINLIIKNLSKSLT	SARS-CoV-2	ORF6	31
126	VIDNEIIVKPNISLC	229E		
127	KIEDLSIRNLQKRLY	HKU1		
128	YVTNEIGLNASVTLK	NL63		
129	YENKLKAKNESSSLC	OC43		
130	MFHLVDFQVTIAEIL	SARS-CoV-2	ORF6	1
131	NVHLKDVTKENQEIL	229E		
132	MHWLIRFIVFVANML	HKU1		
133	MDLLLDDFVTILKSL	NL63		

134	MPFLLDDLVPRAYYL	OC43		
135	VKHVYQLRARSVSPK	SARS-CoV-2	ORF7a	71
136	IKNVNSVRDWLKSLK	229E		
137	VDNVYVTYAGSVWHI	HKU1		
138	VDISYLNRARGSSAA	NL63		
139	NSSILSLCAFSVDPK	OC43		
140	FYSKWYIRVGARKSA	SARS-CoV-2	ORF8	41
141	FISVLDITDAAVKAA	229E		
142	TRSMTYCRVGACEYA	HKU1		
143	ANGFFYIDVGNHRSA	NL63		
144	SPCKELEGVGAKVSA	OC43		
145	DAALALLLLDRLNQL	SARS-CoV-2	N	216
146	DAGHSLTWLWLLCGL	229E		
147	APATGWLLYQLLNGL	HKU1		
148	IIAVELLLLDFKTAV	NL63		
149	DLALKLKGLDAMFFY	OC43		
150	PSGTWLTYTGAIKLD	SARS-CoV-2	N	326
151	PEGCVLTNTGSVVKP	229E		
152	PGNTFITVEAAIELS	HKU1		
153	PSVAVRTYSEAAAQG	NL63		
154	KDVYELRYNGAIRFD	OC43		
155	LLLLDRLNQLESKMS	SARS-CoV-2	N	221
156	ELLLALLAFFLSKHS	229E		
157	WLLPDAAEELASPMK	HKU1		
158	LNLSSELKQLEAKTA	NL63		
159	SLFVDYSNLLHSKVK	OC43		

Table S3: Composition of the Human Coronavirus homologs of SARS-CoV-2 CD4S epitopes (HCoV-S124)

Sort	Sequence	Organism	Protein	Start
1	SLLIVNNATNVVIKV	SARS-CoV-2	S	116
2	GLNKVKYATVVVGST	229E		
3	EDAIIVNDENSSIKV	HKU1		
4	GVFGVNLRTNFTIKG	NL63		
5	SLGFYNPPTNVVSHV	OC43		
6	NNATNVVIKVCEFQF	SARS-CoV-2	S	121
7	NPVSFVVKPVCSSIF	229E		
8	ESQGNVVTSVMESQI	HKU1		
9	NIAFNVVKKGCFTGV	NL63		
10	NPPTNVVSHVNGDWF	OC43		
11	CEFQFCNDPFLGVYY	SARS-CoV-2	S	131
12	ELLQFVTDPTLIVAS	229E		
13	CKFAVCGDGFVPFLL	HKU1		
14	QPFSFSFRDELGVRV	NL63		
15	CQFKDKNLQDLWVLY	OC43		
16	CTFEYVSQPFLMDLE	SARS-CoV-2	S	166
17	EEIEYVHGDALHTLR	229E		
18	CGIKYVAQPTEDVVD	HKU1		
19	DTCFGVSKPNAIDVE	NL63		
20	LIREIVMNASPYDLE	OC43		
21	IGINITRFQTLLALH	SARS-CoV-2	S	231
22	TGVNDAITQTSQALQ	229E		
23	IFKNNTSFPTNIAVE	HKU1		
24	VMNNIVLFLTWLLSM	NL63		
25	IFINNTTYPTNVAVE	OC43		
26	TRFQTLLALHRSYLT	SARS-CoV-2	S	236
27	TPFMILLVALSLCLT	229E		
28	FPKGYVMGLFRSYKT	HKU1		
29	TLFKFLLLLYAIYAL	NL63		
30	TIFNCVYALNNVYLG	OC43		
31	FTVEKGIYQTSNFRV	SARS-CoV-2	S	306
32	FAVESGGYIPSDFAF	229E		
33	FEVEKGVTVDDFVAV	HKU1		
34	FDVVFGHGAGSVVFV	NL63		
35	KRGEKGAYNKDHGRG	OC43		
36	SNFRVQPTESIVRFP	SARS-CoV-2	S	316
37	SNSNYLLEEFDVVFG	229E		
38	YSFGRCPTSSIIKHP	HKU1		
39	SLWRVTAVHSDGMFV	NL63		
40	LLFDVIVAWHVVRDP	OC43		
41	QPTESIVRFPNITNL	SARS-CoV-2	S	321
42	QPVEGVSSFMNVTLD	229E		

43	QPTEDVVDGDVVIRE	HKU1		
44	NNTDSIVIGGVTYQL	NL63		
45	ICSASDMTNPDYTNL	OC43		
46	IVRFPNITNLCPFGE	SARS-CoV-2	S	326
47	CVEMHNKINLCDDPE	229E		
48	AWRFPCAGRKVNFNE	HKU1		
49	CVDLHNKINLCDDPE	NL63		
50	SVVEVVTTSLTPCGY	OC43		
51	CPFGEVFNATRFASV	SARS-CoV-2	S	336
52	FSFGKVNNFVKFGSV	229E		
53	FKFDEPSDATDFIRV	HKU1		
54	STVVEVKSAIVCASV	NL63		
55	LVPQENYSSIRFASV	OC43		
56	VFNATRFASVYAWNR	SARS-CoV-2	S	341
57	VWHAKDFNSLSAEGR	229E		
58	WFNTMLDASAPATGW	HKU1		
59	WFCANQSTSVYSANG	NL63		
60	VKNIPRYASAVAQAF	OC43		
61	SVASQSIIAYTMSLG	SARS-CoV-2	S	686
62	RLHNFSIISGTAFLG	229E		
63	SVATFYIEHYVNRLV	HKU1		
64	SSATDAIIAVELLLL	NL63		
65	SVKSYDSLVYTGVLG	OC43		
66	AYSNNSIAIPTNFTI	SARS-CoV-2	S	706
67	ESAYMPIADPTHFDI	229E		
68	VGGLYEIKIPTNFTI	HKU1		
69	ASGVFGVNLRTNFTI	NL63		
70	VGGLYEIQIPSEFTI	OC43		
71	NLLLQYGSFCTQLNR	SARS-CoV-2	S	751
72	LLLWESGKAKPPLNR	229E		
73	DLLSEYGTFCDNINS	HKU1		
74	NLLKQYTSACKTIED	NL63		
75	SQLVEYGSFCDNINA	OC43		
76	TQLNRALTGIAVEQD	SARS-CoV-2	S	761
77	VMLQIQLTGILDGDY	229E		
78	KLITTACNGISVTQT	HKU1		
79	NQLRLAFLGASVTED	NL63		
80	TILNTACGVFEVDDT	OC43		
81	VFAQVKQIYKTPPIK	SARS-CoV-2	S	781
82	VVGGTIQILASVPEK	229E		
83	CNAQEQQIYFFEGVA	HKU1		
84	VTEDVKFAASTGVID	NL63		
85	VSATVLQNNELMPAK	OC43		
86	NFSQILPDPSKPSKR	SARS-CoV-2	S	801
87	NGSNILEAFTKPVFI	229E		

88	NFVALIPDYAKILVN	HKU1		
89	YFSQLLCEPIKLVNS	NL63		
90	NIEAWLNDKSVPSPL	OC43		
91	KPSKRSFIEDLLFNK	SARS-CoV-2	S	811
92	RVAGRSAIEDILFSK	229E		
93	GSSSRSFFEDLLFDK	HKU1		
94	RIAGRSALEDLLFSK	NL63		
95	KASSRSAIEDLLFDK	OC43		
96	SFIEDLLFNKVTLAD	SARS-CoV-2	S	816
97	SAIEDILFSKLVTSG	229E		
98	SFFEDLLFDKVKLSD	HKU1		
99	SALEDLLFSKVVTSG	NL63		
100	SAIEDLLFDKVKLSD	OC43		
101	CAQKFNGLTVLPPLL	SARS-CoV-2	S	851
102	CAQYYNGIMVLPGVA	229E		
103	CVQSFNGIKVLPPIL	HKU1		
104	CAQYYNGIMVLPGVA	NL63		
105	CVQSYKGIKVLPPLL	OC43		
106	AQYTSALLAGTITSG	SARS-CoV-2	S	871
107	AWYFLAMLTGLLPSL	229E		
108	LLCRVTLGDFTIMSG	HKU1		
109	FSPFNSLLCGDIVSG	NL63		
110	ISSTVRLQAGTATEY	OC43		
111	WTFGAGAALQIPFAM	SARS-CoV-2	S	886
112	TTQQAGAGIKYFCGM	229E		
113	MLHGGGVAKAIAVAA	HKU1		
114	GTFESAAAGTFVLDM	NL63		
115	ETFTVCADGFMPFLL	OC43		
116	AQALNTLVKQLSSNF	SARS-CoV-2	S	956
117	GNSLNHLTSQLRQNF	229E		
118	AQALNSLLQQLFNKF	HKU1		
119	GSALNHLTSQLRHNF	NL63		
120	AEALNNLLQQLSNRF	OC43		
121	GAISSVLNDILSRLD	SARS-CoV-2	S	971
122	QAISSSIQAIYDRLD	229E		
123	GAISSSLQEILSRLD	HKU1		
124	SAMHSLLFGMLRRLD	NL63		
125	GAISASLQEILSRLD	OC43		
126	VQIDRLITGRLQSLQ	SARS-CoV-2	S	991
127	QQVDRLITGRLAALN	229E		
128	VQIDRLINGRLTALN	HKU1		
129	QQVDRLITGRLAALN	NL63		
130	AQIDRLINGRLTALN	OC43		
131	APHGVVFLHVTYVPA	SARS-CoV-2	S	1056
132	APEGLVFLHTVLLPT	229E		

133	APYGLLFMHFSYKPI	HKU1		
134	APDGLLFLHTVLLPT	NL63		
135	APYGLYFIHFSYVPT	OC43		
136	ELDKYFKNHTSPDVD	SARS-CoV-2	S	1151
137	ALDKLYKVFGSPVMT	229E		
138	ELSHWFKNQTSIAPN	HKU1		
139	EFRDYFNNNTDSIVI	NL63		
140	ELDQWFKNQTSVAPD	OC43		
141	GINASVVNIQKEIDR	SARS-CoV-2	S	1171
142	GNQTLFCNIMKFSDR	229E		
143	LIPRSYYLIQSGIFF	HKU1		
144	GLNASVTLKICKFSR	NL63		
145	GIFAKVKNTKVIKDR	OC43		
146	LNEVAKNLNESLIDL	SARS-CoV-2	S	1186
147	WNGVIKNVNSVRDWL	229E		
148	IQESIKSLNNSYINL	HKU1		
149	LFVVALFIGVSFIDY	NL63		
150	LQEAIKVLNQSYINL	OC43		
151	YEQYIKWPWYIWLGF	SARS-CoV-2	S	1206
152	VETYIKWPWWVWLCI	229E		
153	YEMYVKWPWYVWLLI	HKU1		
154	FENYIKWPWWVWLII	NL63		
155	YEYYVKWPWYVWLLI	OC43		

Table S4: Unexposed donor cohort utilized to verify crossreactivity.

Donor ID	Gender	Age[a]	Blood draw
1572	F	32	2015
1578	F	25	2015
1598	F	52	2015
1686	F	52	2015
1690	M	41	2015
2104	F	26	2015
2105	F	27	2015
2109	M	31	2015
2122	Unknown	Unknown	2015
2123	Unknown	Unknown	2015
2132	F	54	2015
2144	F	50	2015
2198	F	34	2015
2228	M	34	2015
1577	F	67	2017
1568	M	60	2020
1584	M	35	2020
1767	M	60	2020
2033	F	39	2020
2511	M	32	2020
2718	F	59	2020
3804	M	27	2020
3986	F	25	2020
4218	M	38	2020
4761	F	27	2020

[a]Age at the time of the blood draw.

Table S5: COVID-19 donor cohort utilized to verify crossreactivity.

Donor ID	Gender	Age[a]	Blood draw
4801	M	58	2020
4837	F	28	2020
4842	M	49	2020
4853	M	49	2020
4795	M	39	2020
4797	F	62	2020
4863	F	44	2020
4864	F	32	2020
4865	M	34	2020
4879	M	63	2020
4880	F	46	2020
4881	M	38	2020
4883	F	57	2020
4884	M	57	2020
4887	F	60	2020
4924	F	42	2020
4927	F	34	2020
4928	M	50	2020
4929	M	57	2020
4935	M	42	2020

[a]Age at the time of the blood draw.

Table S6: HLA types of the donor cohort utilized in epitope identification studies.

Donor ID	Gender	Age[a]	Blood draw	A	A	B	B	C	C	DPB1	DPB1	DQA1	DQA1	DQB1	DQB1	DRB1	DRB1	DRB 3/4/5	DRB 3/4/5
1570	F	44	2015	29:02	68:05	15:15	44:03	03:04	16:01	03:01	11:01	ND	ND	02:02	03:02	04:10	07:01	01:01	01:01
1986	F	47	2015	24:02	26:01	07:02	07:02	07:02	07:02	02:01	06:01	01:01	02:01	02:02	05:01	01:03	07:01	01:01	-
2079	F	43	2015	11:01	25:01	18:01	35:01	04:01	12:03	04:01	04:01	01:01	01:02	05:01	06:02	01:01	15:01	01:01	-
2085	M	46	2015	03:01	32:01	07:02	44:02	05:01	07:02	04:01	06:01	01:02	06:01	03:01	06:02	08:03	15:01	01:01	-
2086	F	33	2015	01:01	02:06	37:01	52:01	04:01	06:02	02:01	04:02	01:01	03:01	03:02	05:01	04:04	10:01	01:01	-
2095	F	26	2015	33:03	33:03	58:01	58:01	03:02	03:02	04:01	04:01	05:01	05:01	02:01	02:01	03:01	03:81	02:02	02:02
2117	Unknown	Unknown	2015	02:01	29:02	15:17	44:03	07:01	16:01	03:01	04:01	01:02	01:02	06:02	06:04	13:02	15:01	03:01	01:01
2130	F	51	2015	02:01	30:01	13:02	15:01	03:03	06:02	03:01	04:01	01:03	02:01	02:02	06:03	07:01	13:01	02:02	01:01
2208	M	48	2015	23:01	29:02	15:01	44:03	04:01	16:01	09:01	11:01	01:01	02:01	02:02	05:01	01:01	07:01	01:01	-
2209	F	24	2015	26:01	33:03	15:01	56:01	03:03	04:01	05:01	05:01	03:01	03:01	03:03	04:02	09:01	09:01	01:01	01:01
2246	M	23	2015	02:01	36:01	35:01	53:01	04:01	16:01	01:01	02:01	01:02	02:01	06:02	02:02	11:01	13:03	02:02	02:02
1565	M	25	2016	02:03	24:02	15:02	38:02	07:02	08:01	05:01	31:01	ND b	ND	05:02	05:02	14:01	16:02	02:02	01:01
1592	F	24	2017	02:03	24:02	40:01	40:06	04:03	08:01	03:01	02:01	ND	ND	03:01	06:01	08:03	12:02	03:01	- c
1616	M	45	2017	02:01	68:02	14:02	39:01	08:02	12:03	02:01	04:01	ND	ND	03:01	03:01	11:02	13:03	01:01	02:02
2184	F	29	2017	03:01	29:02	44:03	51:01	14:02	16:01	02:01	11:01	01:01	02:01	02:02	05:01	01:01	07:01	01:01	-
2234	F	20	2017	29:02	29:02	44:03	44:03	16:01	16:01	11:01	11:01	02:01	02:01	02:02	02:02	07:01	07:01	01:01	01:01
2909	F	66	2017	02:01	11:01	35:01	35:03	04:01	04:01	02:01	04:01	01:01	05:01	03:01	05:01	01:01	11:01	02:02	-
1767	F	21	2018	02:01	11:01	35:01	35:03	04:01	04:01	02:01	04:01	01:01	05:01	03:01	05:01	01:01	11:01	02:02	-

a. Age at the time of the blood draw.

b. ND indicates locus not typed.

c. A dash ("-") indicates no allele expressed.

Table S7: Antibodies utilized in the intracellular cytokine staining (ICS) assay.

Membrane Antibody	Fluorochrome	Clone/vendor/catalog	Dilution
CD4	Pacific Blue	RPA-T4/BD/558116	1:50
CD14	V500	M5E2/BD/561391	1:50
CD19	V500	HIB19/BD/561121	1:50
LIVE/DEAD	ef506/Aqua	Thermo Fisher/65-0866-18	1:200
CD8	BV650	RPA-T8/Biolegend/301042	1:50
IFNγ	FITC	4S.B3/Thermo Fisher/11-7319-82	1:100
CD3	Alexa Fluor 700	UCHT1/Thermo Fisher/56-0038-42	1:50

Table S8: Antibodies utilized in the activation induced markers (AIM) assay.

Membrane Antibody	Fluorochrome	Clone/vendor/catalog	Dilution
CD45RA	BV421	HI100/Biolegend/304130	1:100
CD14	V500	M5E2/BD/561391	1:50
CD19	V500	HIB19/BD/561121	1:50
Live/Dead	ef506/Aqua	Thermo Fisher/65-0866-18	1:200
CD8	BV650	RPA-T8/BioLegend/301042	1:50
CD4	BV605	RPA-T4/BD/562658	1:25
CCR7	FITC	G043H7/Biolegend/353216	1:100
CD69	PE	FN50/BD/555531	1:10
OX40	PE-Cy7	Ber-ACT35/Biolegend/350012	1:50
CD137	APC	4B4-1/BioLegend/309810	1:50
CD3	AF700	UCHT1/Thermo Fisher/56-0038-42	1:50

References and Notes

1. E. Dong, H. Du, L. Gardner, An interactive web-based dashboard to track COVID-19 in real time. *Lancet Infect. Dis.* **20**, 533–534 (2020). doi:10.1016/S1473-3099(20)30120-1 Medline

2. C. Huang, Y. Wang, X. Li, L. Ren, J. Zhao, Y. Hu, L. Zhang, G. Fan, J. Xu, X. Gu, Z. Cheng, T. Yu, J. Xia, Y. Wei, W. Wu, X. Xie, W. Yin, H. Li, M. Liu, Y. Xiao, H. Gao, L. Guo, J. Xie, G. Wang, R. Jiang, Z. Gao, Q. Jin, J. Wang, B. Cao, Clinical features of patients infected with 2019 novel coronavirus in Wuhan, China. *Lancet* **395**, 497–506 (2020). doi:10.1016/S0140-6736(20)30183-5 Medline

3. N. Le Bert, A. T. Tan, K. Kunasegaran, C. Y. L. Tham, M. Hafezi, A. Chia, M. H. Y. Chng, M. Lin, N. Tan, M. Linster, W. N. Chia, M. I.-C. Chen, L.-F. Wang, E. E. Ooi, S. Kalimuddin, P. A. Tambyah, J. G.-H. Low, Y.-J. Tan, A. Bertoletti, SARS-CoV-2-specific T cell immunity in cases of COVID-19 and SARS, and uninfected controls. *Nature* (2020). doi:10.1038/s41586-020-2550-z Medline

4. A. Grifoni, D. Weiskopf, S. I. Ramirez, J. Mateus, J. M. Dan, C. R. Moderbacher, S. A. Rawlings, A. Sutherland, L. Premkumar, R. S. Jadi, D. Marrama, A. M. de Silva, A. Frazier, A. F. Carlin, J. A. Greenbaum, B. Peters, F. Krammer, D. M. Smith, S. Crotty, A. Sette, Targets of T cell responses to SARS-CoV-2 coronavirus in humans with COVID-19 disease and unexposed individuals. *Cell* **181**, 1489–1501.e15 (2020). doi:10.1016/j.cell.2020.05.015 Medline

5. B. J. Meckiff, C. Ramírez-Suástegui, V. Fajardo, S. J. Chee, A. Kusnadi, H. Simon, A. Grifoni, E. Pelosi, D. Weiskopf, A. Sette, F. Ay, G. Seumois, C. H. Ottensmeier, P. Vijayanand, Single-cell transcriptomic analysis of SARS-CoV-2 reactive CD4 $^{+}$ T cells. *bioRxiv* 2020.06.12.148916 (2020). Medline

6. D. Weiskopf, K. S. Schmitz, M. P. Raadsen, A. Grifoni, N. M. A. Okba, H. Endeman, J. P. C. van den Akker, R. Molenkamp, M. P. G. Koopmans, E. C. M. van Gorp, B. L. Haagmans, R. L. de Swart, A. Sette, R. D. de Vries, Phenotype and kinetics of SARS-CoV-2-specific T cells in COVID-19 patients with acute respiratory distress syndrome. *Sci. Immunol.* **5**, eabd2071 (2020). doi:10.1126/sciimmunol.abd2071 Medline

7. J. Braun, L. Loyal, M. Frentsch, D. Wendisch, P. Georg, F. Kurth, S. Hippenstiel, M. Dingeldey, B. Kruse, F. Fauchere, E. Baysal, M. Mangold, L. Henze, R. Lauster, M. Mall, K. Beyer, J. Roehmel, J. Schmitz, S. Miltenyi, M. A. Mueller, M. Witzenrath, N. Suttorp, F. Kern, U. Reimer, H. Wenschuh, C. Drosten, V. M. Corman, C. Giesecke-Thiel, L.-E. Sander, A. Thiel, Presence of SARS-CoV-2 reactive T cells in COVID-19 patients and healthy donors. medRxiv 2020.2004.2017.20061440 [Preprint]. 22 April 2020; https://doi.org/10.1101/2020.04.17.20061440.

8. Y. Peng, A. J. Mentzer, G. Liu, X. Yao, Z. Yin, D. Dong, W. Dejnirattisai, T. Rostron, P. Supasa, C. Liu, C. Lopez-Camacho, J. Slon-Campos, Y. Zhao, D. Stuart, G. Paeson, J. Grimes, F. Antson, O. W. Bayfield, D. E. Hawkins, D. S. Ker, L. Turtle, K. Subramaniam, P. Thomson, P. Zhang, C. Dold, J. Ratcliff, P. Simmonds, T. de Silva, P. Sopp, D. Wellington, U. Rajapaksa, Y. L. Chen, M. Salio, G. Napolitani, W. Paes, P. Borrow, B. Kessler, J. W. Fry, N. F. Schwabe, M. G. Semple, K. J. Baillie, S. Moore, P. J. Openshaw, A. Ansari, S. Dunachie, E. Barnes, J. Frater, G. Kerr, P. Goulder, T.

Lockett, R. Levin, R. J. Cornall, C. Conlon, P. Klenerman, A. McMichael, G. Screaton, J. Mongkolsapaya, J. C. Knight, G. Ogg, T. Dong, Broad and strong memory CD4 $^{+}$ and CD8 $^{+}$ T cells induced by SARS-CoV-2 in UK convalescent COVID-19 patients. *bioRxiv* 2020.06.05.134551 (2020). Medline

9. L. Kuri-Cervantes, M. B. Pampena, W. Meng, A. M. Rosenfeld, C. A. G. Ittner, A. R. Weisman, R. Agyekum, D. Mathew, A. E. Baxter, L. Vella, O. Kuthuru, S. Apostolidis, L. Bershaw, J. Dougherty, A. R. Greenplate, A. Pattekar, J. Kim, N. Han, S. Gouma, M. E. Weirick, C. P. Arevalo, M. J. Bolton, E. C. Goodwin, E. M. Anderson, S. E. Hensley, T. K. Jones, N. S. Mangalmurti, E. T. Luning Prak, E. J. Wherry, N. J. Meyer, M. R. Betts, Immunologic perturbations in severe COVID-19/SARS-CoV-2 infection. *bioRxiv* 2020.05.18.101717 (2020). Medline

10. I. Thevarajan, T. H. O. Nguyen, M. Koutsakos, J. Druce, L. Caly, C. E. van de Sandt, X. Jia, S. Nicholson, M. Catton, B. Cowie, S. Y. C. Tong, S. R. Lewin, K. Kedzierska, Breadth of concomitant immune responses prior to patient recovery: A case report of non-severe COVID-19. *Nat. Med.* **26**, 453–455 (2020). doi:10.1038/s41591-020-0819-2 Medline

11. L. Rodriguez, P. Pekkarinen, L. Kanth Tadepally, Z. Tan, C. Rosat Consiglio, C. Pou, Y. Chen, C. Habimana Mugabo, A. Nguyen Quoc, K. Nowlan, T. Strandin, L. Levanov, J. Mikes, J. Wang, A. Kantele, J. Hepojoki, O. Vapalahti, S. Heinonen, E. Kekalainen, P. Brodin, Systems-level immunomonitoring from acute to recovery phase of severe COVID-19. medRxiv 2020.2006.2003.20121582 [Preprint]. 7 June 2020; https://doi.org/10.1101/2020.06.03.20121582.

12. J. Liu, S. Li, J. Liu, B. Liang, X. Wang, H. Wang, W. Li, Q. Tong, J. Yi, L. Zhao, L. Xiong, C. Guo, J. Tian, J. Luo, J. Yao, R. Pang, H. Shen, C. Peng, T. Liu, Q. Zhang, J. Wu, L. Xu, S. Lu, B. Wang, Z. Weng, C. Han, H. Zhu, R. Zhou, H. Zhou, X. Chen, P. Ye, B. Zhu, L. Wang, W. Zhou, S. He, Y. He, S. Jie, P. Wei, J. Zhang, Y. Lu, W. Wang, L. Zhang, L. Li, F. Zhou, J. Wang, U. Dittmer, M. Lu, Y. Hu, D. Yang, X. Zheng, Longitudinal characteristics of lymphocyte responses and cytokine profiles in the peripheral blood of SARS-CoV-2 infected patients. *EBioMedicine* **55**, 102763 (2020). doi:10.1016/j.ebiom.2020.102763 Medline

13. D. Mathew, J. R. Giles, A. E. Baxter, D. A. Oldridge, A. R. Greenplate, J. E. Wu, C. Alanio, L. Kuri-Cervantes, M. B. Pampena, K. D'Andrea, S. Manne, Z. Chen, Y. J. Huang, J. P. Reilly, A. R. Weisman, C. A. G. Ittner, O. Kuthuru, J. Dougherty, K. Nzingha, N. Han, J. Kim, A. Pattekar, E. C. Goodwin, E. M. Anderson, M. E. Weirick, S. Gouma, C. P. Arevalo, M. J. Bolton, F. Chen, S. F. Lacey, H. Ramage, S. Cherry, S. E. Hensley, S. A. Apostolidis, A. C. Huang, L. A. Vella, M. R. Betts, N. J. Meyer, E. J. Wherry; UPenn COVID Processing Unit, Deep immune profiling of COVID-19 patients reveals distinct immunotypes with therapeutic implications. *Science* eabc8511 (2020). doi:10.1126/science.abc8511 Medline

14. M. E. Killerby, H. M. Biggs, A. Haynes, R. M. Dahl, D. Mustaquim, S. I. Gerber, J. T. Watson, Human coronavirus circulation in the United States 2014-2017. *J. Clin. Virol.* **101**, 52–56 (2018). doi:10.1016/j.jcv.2018.01.019 Medline

15. G. J. Gorse, G. B. Patel, J. N. Vitale, T. Z. O'Connor, Prevalence of antibodies to four human coronaviruses is lower in nasal secretions than in serum. *Clin. Vaccine Immunol.* **17**, 1875–1880 (2010). doi:10.1128/CVI.00278-10 Medline

16. E. E. Walsh, J. H. Shin, A. R. Falsey, Clinical impact of human coronaviruses 229E and OC43 infection in diverse adult populations. *J. Infect. Dis.* **208**, 1634–1642 (2013). doi:10.1093/infdis/jit393 Medline

17. S. Nickbakhsh, A. Ho, D. F. P. Marques, J. McMenamin, R. N. Gunson, P. R. Murcia, Epidemiology of seasonal coronaviruses: Establishing the context for the emergence of coronavirus disease 2019. *J. Infect. Dis.* **222**, 17–25 (2020). doi:10.1093/infdis/jiaa185 Medline

18. S. M. Kissler, C. Tedijanto, E. Goldstein, Y. H. Grad, M. Lipsitch, Projecting the transmission dynamics of SARS-CoV-2 through the postpandemic period. *Science* **368**, 860–868 (2020). doi:10.1126/science.abb5793 Medline

19. D. Weiskopf, M. A. Angelo, A. Grifoni, P. H. O'Rourke, J. Sidney, S. Paul, A. D. De Silva, E. Phillips, S. Mallal, S. Premawansa, G. Premawansa, A. Wijewickrama, B. Peters, A. Sette, HLA-DRB1 alleles are associated with different magnitudes of dengue virus-specific CD4+ T-cell responses. *J. Infect. Dis.* **214**, 1117–1124 (2016). doi:10.1093/infdis/jiw309 Medline

20. C. Oseroff, J. Sidney, M. F. Kotturi, R. Kolla, R. Alam, D. H. Broide, S. I. Wasserman, D. Weiskopf, D. M. McKinney, J. L. Chung, A. Petersen, H. Grey, B. Peters, A. Sette, Molecular determinants of T cell epitope recognition to the common Timothy grass allergen. *J. Immunol.* **185**, 943–955 (2010). doi:10.4049/jimmunol.1000405 Medline

21. D. Weiskopf, C. Cerpas, M. A. Angelo, D. J. Bangs, J. Sidney, S. Paul, B. Peters, F. P. Sanches, C. G. T. Silvera, P. R. Costa, E. G. Kallas, L. Gresh, A. D. de Silva, A. Balmaseda, E. Harris, A. Sette, Human CD8+ T cell responses against the 4 Dengue virus serotypes are associated with distinct patterns of protein targets. *J. Infect. Dis.* **212**, 1743–1751 (2015). doi:10.1093/infdis/jiv289 Medline

22. H. Voic, R. D. de Vries, J. Sidney, P. Rubiro, E. Moore, E. J. Phillips, S. Mallal, B. Schwan, D. Weiskopf, A. Grifoni, A. Sette, Identification and characterization of CD4+ T cell epitopes after Shingrix vaccination. bioRxiv 2020/227082 [Preprint]. 29 July 2020; https://doi.org/10.1101/2020.07.29.227082.

23. D. R. Madden, The three-dimensional structure of peptide-MHC complexes. *Annu. Rev. Immunol.* **13**, 587–622 (1995). doi:10.1146/annurev.iy.13.040195.003103 Medline

24. R. T. Carson, K. M. Vignali, D. L. Woodland, D. A. Vignali, T cell receptor recognition of MHC class II-bound peptide flanking residues enhances immunogenicity and results in altered TCR V region usage. *Immunity* **7**, 387–399 (1997). doi:10.1016/S1074-7613(00)80360-X Medline

25. J. M. Dan, C. S. Lindestam Arlehamn, D. Weiskopf, R. da Silva Antunes, C. Havenar-Daughton, S. M. Reiss, M. Brigger, M. Bothwell, A. Sette, S. Crotty, A cytokine-independent approach to identify antigen-specific human germinal center T follicular helper cells and rare antigen-specific CD4+ T cells in blood. *J. Immunol.* **197**, 983–993 (2016). doi:10.4049/jimmunol.1600318 Medline

26. C. Havenar-Daughton, S. M. Reiss, D. G. Carnathan, J. E. Wu, K. Kendric, A. Torrents de la Peña, S. P. Kasturi, J. M. Dan, M. Bothwell, R. W. Sanders, B. Pulendran, G. Silvestri, S. Crotty, Cytokine-independent detection of antigen-specific germinal center T follicular helper cells in immunized nonhuman primates using a live cell activation-induced marker technique. *J. Immunol.* **197**, 994–1002 (2016). doi:10.4049/jimmunol.1600320 Medline

27. S. Reiss, A. E. Baxter, K. M. Cirelli, J. M. Dan, A. Morou, A. Daigneault, N. Brassard, G. Silvestri, J.-P. Routy, C. Havenar-Daughton, S. Crotty, D. E. Kaufmann, Comparative analysis of activation induced marker (AIM) assays for sensitive identification of antigen-specific CD4 T cells. *PLOS ONE* **12**, e0186998 (2017). doi:10.1371/journal.pone.0186998 Medline

28. A. Vatti, D. M. Monsalve, Y. Pacheco, C. Chang, J.-M. Anaya, M. E. Gershwin, Original antigenic sin: A comprehensive review. *J. Autoimmun.* **83**, 12–21 (2017). doi:10.1016/j.jaut.2017.04.008 Medline

29. K. Kadkhoda, COVID-19: An immunopathological view. *MSphere* **5**, e00344-20 (2020). doi:10.1128/mSphere.00344-20 Medline

30. F. Sallusto, A. Langenkamp, J. Geginat, A. Lanzavecchia, Functional subsets of memory T cells identified by CCR7 expression. *Curr. Top. Microbiol. Immunol.* **251**, 167–171 (2000). doi:10.1007/978-3-642-57276-0_21 Medline

31. A. Grifoni, H. Voic, S. K. Dhanda, C. K. Kidd, J. D. Brien, S. Buus, A. Stryhn, A. P. Durbin, S. Whitehead, S. A. Diehl, A. D. De Silva, A. Balmaseda, E. Harris, D. Weiskopf, A. Sette, T cell responses induced by attenuated flavivirus vaccination are specific and show limited cross-reactivity with other flavivirus species. *J. Virol.* **94**, e00089-20 (2020). doi:10.1128/JVI.00089-20 Medline

32. E. J. Hensen, B. G. Elferink, Primary sensitisation and restimulation of human lymphocytes with soluble antigen in vitro. *Nature* **277**, 223–225 (1979). doi:10.1038/277223a0 Medline

33. L. Premkumar, B. Segovia-Chumbez, R. Jadi, D. R. Martinez, R. Raut, A. Markmann, C. Cornaby, L. Bartelt, S. Weiss, Y. Park, C. E. Edwards, E. Weimer, E. M. Scherer, N. Rouphael, S. Edupuganti, D. Weiskopf, L. V. Tse, Y. J. Hou, D. Margolis, A. Sette, M. H. Collins, J. Schmitz, R. S. Baric, A. M. de Silva, The receptor binding domain of the viral spike protein is an immunodominant and highly specific target of antibodies in SARS-CoV-2 patients. *Sci. Immunol.* **5**, eabc8413 (2020). doi:10.1126/sciimmunol.abc8413 Medline

34. M. Yuan, N. C. Wu, X. Zhu, C. D. Lee, R. T. Y. So, H. Lv, C. K. P. Mok, I. A. Wilson, A highly conserved cryptic epitope in the receptor binding domains of SARS-CoV-2 and SARS-CoV. *Science* **368**, 630–633 (2020). doi:10.1126/science.abb7269 Medline

35. A. Z. Wec, D. Wrapp, A. S. Herbert, D. P. Maurer, D. Haslwanter, M. Sakharkar, R. K. Jangra, M. E. Dieterle, A. Lilov, D. Huang, L. V. Tse, N. V. Johnson, C.-L. Hsieh, N. Wang, J. H. Nett, E. Champney, I. Burnina, M. Brown, S. Lin, M. Sinclair, C. Johnson, S. Pudi, R. Bortz 3rd, A. S. Wirchnianski, E. Laudermilch, C. Florez, J. M. Fels, C. M. O'Brien, B. S. Graham, D. Nemazee, D. R. Burton, R. S. Baric, J. E. Voss, K. Chandran, J. M. Dye, J. S. McLellan, L. M. Walker, Broad neutralization of SARS-related viruses

by human monoclonal antibodies. *Science* eabc7424 (2020). doi:10.1126/science.abc7424 Medline

36. A. Sette, S. Crotty, Pre-existing immunity to SARS-CoV-2: The knowns and unknowns. *Nat. Rev. Immunol.* **20**, 457–458 (2020). doi:10.1038/s41577-020-0389-z Medline

37. A. Grifoni, J. Sidney, Y. Zhang, R. H. Scheuermann, B. Peters, A. Sette, Candidate targets for immune responses to 2019-Novel Coronavirus (nCoV): Sequence homology- and bioinformatic-based predictions. bioRxiv 2020.02.12.946087 [Preprint]. 16 March 2020; https://doi.org/10.1101/2020.02.12.946087.

38. F. Amanat, D. Stadlbauer, S. Strohmeier, T. H. O. Nguyen, V. Chromikova, M. McMahon, K. Jiang, G. A. Arunkumar, D. Jurczyszak, J. Polanco, M. Bermudez-Gonzalez, G. Kleiner, T. Aydillo, L. Miorin, D. S. Fierer, L. A. Lugo, E. M. Kojic, J. Stoever, S. T. H. Liu, C. Cunningham-Rundles, P. L. Felgner, T. Moran, A. García-Sastre, D. Caplivski, A. C. Cheng, K. Kedzierska, O. Vapalahti, J. M. Hepojoki, V. Simon, F. Krammer, A serological assay to detect SARS-CoV-2 seroconversion in humans. *Nat. Med.* **26**, 1033–1036 (2020). doi:10.1038/s41591-020-0913-5 Medline

39. J. Greenbaum, J. Sidney, J. Chung, C. Brander, B. Peters, A. Sette, Functional classification of class II human leukocyte antigen (HLA) molecules reveals seven different supertypes and a surprising degree of repertoire sharing across supertypes. *Immunogenetics* **63**, 325–335 (2011). doi:10.1007/s00251-011-0513-0 Medline

40. S. Carrasco Pro, J. Sidney, S. Paul, C. Lindestam Arlehamn, D. Weiskopf, B. Peters, A. Sette, Automatic generation of validated specific epitope sets. *J. Immunol. Res.* **2015**, 763461 (2015). doi:10.1155/2015/763461 Medline

41. D. Hinz, G. Seumois, A. M. Gholami, J. A. Greenbaum, J. Lane, B. White, D. H. Broide, V. Schulten, J. Sidney, P. Bakhru, C. Oseroff, E. Wambre, E. A. James, W. W. Kwok, B. Peters, P. Vijayanand, A. Sette, Lack of allergy to timothy grass pollen is not a passive phenomenon but associated with the allergen-specific modulation of immune reactivity. *Clin. Exp. Allergy* **46**, 705–719 (2016). doi:10.1111/cea.12692 Medline

42. C. S. Lindestam Arlehamn, D. M. McKinney, C. Carpenter, S. Paul, V. Rozot, E. Makgotlho, Y. Gregg, M. van Rooyen, J. D. Ernst, M. Hatherill, W. A. Hanekom, B. Peters, T. J. Scriba, A. Sette, A quantitative analysis of complexity of human pathogen-specific CD4 T cell responses in healthy *M. tuberculosis* infected South Africans. *PLOS Pathog.* **12**, e1005760 (2016). doi:10.1371/journal.ppat.1005760 Medline

43. T. Bancroft, M. B. C. Dillon, R. da Silva Antunes, S. Paul, B. Peters, S. Crotty, C. S. Lindestam Arlehamn, A. Sette, Th1 versus Th2 T cell polarization by whole-cell and acellular childhood pertussis vaccines persists upon re-immunization in adolescence and adulthood. *Cell. Immunol.* **304-305**, 35–43 (2016). doi:10.1016/j.cellimm.2016.05.002 Medline

44. R. da Silva Antunes, S. Paul, J. Sidney, D. Weiskopf, J. M. Dan, E. Phillips, S. Mallal, S. Crotty, A. Sette, C. S. Lindestam Arlehamn, Definition of human epitopes recognized in tetanus toxoid and development of an assay strategy to detect ex vivo tetanus CD4+ T cell responses. *PLOS ONE* **12**, e0169086 (2017). doi:10.1371/journal.pone.0169086 Medline

45. A. Elong Ngono, H.-W. Chen, W. W. Tang, Y. Joo, K. King, D. Weiskopf, J. Sidney, A. Sette, S. Shresta, Protective role of cross-reactive CD8 T cells against Dengue virus infection. *EBioMedicine* **13**, 284–293 (2016). doi:10.1016/j.ebiom.2016.10.006 Medline

46. A. Grifoni, M. A. Angelo, B. Lopez, P. H. O'Rourke, J. Sidney, C. Cerpas, A. Balmaseda, C. G. T. Silveira, A. Maestri, P. R. Costa, A. P. Durbin, S. A. Diehl, E. Phillips, S. Mallal, A. D. De Silva, G. Nchinda, C. Nkenfou, M. H. Collins, A. M. de Silva, M. Q. Lim, P. A. Macary, F. Tatullo, T. Solomon, V. Satchidanandam, A. Desai, V. Ravi, J. Coloma, L. Turtle, L. Rivino, E. G. Kallas, B. Peters, E. Harris, A. Sette, D. Weiskopf, Global assessment of Dengue virus-specific $CD4^+$ T cell responses in Dengue-endemic areas. *Front. Immunol.* **8**, 1309 (2017). doi:10.3389/fimmu.2017.01309 Medline

47. D. Hinz, C. Oseroff, J. Pham, J. Sidney, B. Peters, A. Sette, Definition of a pool of epitopes that recapitulates the T cell reactivity against major house dust mite allergens. *Clin. Exp. Allergy* **45**, 1601–1612 (2015). doi:10.1111/cea.12507 Medline